Rivista Italiana di Paleontologia e Stratigrafia
(*Research in Paleontology and Stratigraphy*)
vol. 132(1): 59-86. **March 2026**
DOI: https://doi.org/10.54103/2039-4942/29019

EARLY DELPHINIDA (CETACEA, ODONTOCETI) FROM THE MIOCENE OF THE SOUTHERN NORTH SEA BASIN

PIETER VAN ROMPAEY[1,2,*], OLIVIER LAMBERT[3], MARK BOSSELAERS[3,4] & STEPHEN LOUWYE[2]

[1]Department of Earth and Environmental Sciences, Division of Geology, KU Leuven, Celestijnenlaan 200E, B-3001 Leuven-Heverlee, Belgium. E-mail: pieter.v.r22@gmail.com
[2]Department of Geology, Ghent University, Krijgslaan 281/S8, B-9000 Ghent, Belgium. E-mail: stephen.louwye@ugent.be
[3]D.O. Terre & Histoire de la Vie, Institut royal des Sciences naturelles de Belgique, rue Vautier 29, B-1000 Brussels, Belgium. E-mail: olambert@naturalsciences.be
[4]Koninklijk Zeeuwsch Genootschap der Wetenschappen, Koudsteensedijk 7, NL-4331, Middelburg, The Netherlands. E-mail: mark.bosselaers@telenet.be
*Corresponding author.

Associate Editor: Giorgio Carnevale.

To cite this article: Van Rompaey P., Lambert O., Bosselaers M. & Louwye S. (2026) - Early Delphinida (Cetacea, Odontoceti) from the Miocene of the southern North Sea Basin. *Rivista Italiana di Paleontologia e Stratigrafia*, vol. 132(1): 59-86.

Keywords: Kentriodontidae; *Kentriodon*; *Brevirostrodelphis*; Berchem Formation; Antwerpen Member; Langhian; Antwerp; Belgium.

Abstract: The earliest delphinidans (Cetacea, Odontoceti, Delphinida) first appear in the fossil record in the upper Oligocene, but are predominantly known from the Miocene. During the excavation of a series of construction pits in Antwerp (northern Belgium), two fragmentary early delphinidan crania were collected from lower Middle Miocene deposits of the Antwerpen Member (Berchem Formation). Both specimens show strong morphological similarities to *Brevirostrodelphis dividum*, originally described from the Miocene Calvert Formation of the U.S. Atlantic Coastal Plain. They are here identified as *Brevirostrodelphis* aff. *B. dividum* and *Brevirostrodelphis* sp., representing the first unambiguous records of this genus from the eastern side of the North Atlantic. In addition, the historical type specimen of *Phocaenopsis scheynensis*, collected in the early 1860s in the Antwerp area, most likely from Lower to Middle Miocene strata, is here redescribed and its systematic status is reassessed. It is here re-identified as *Kentriodon* sp. due to its strong morphological similarities with *Kentriodon pernix,* another early delphinidan originally described from the Calvert Formation of the U.S. Atlantic Coastal Plain. This specimen thus represents the third description of cranial material of *Kentriodon* from the North Sea Basin and the fourth from the eastern side of the North Atlantic. Based on the preponderance of juvenile specimens preserved, the southern North Sea Basin is herein tentatively hypothesized to potentially have served as a nursing ground for, or was favoured by relatively young individuals for several early delphinidan taxa during the Miocene.

Received: June 11, 2025; accepted: January 13, 2026

Introduction

The extant members of the odontocete (toothed whales) infraorder Delphinida include the 'river dolphin' families Pontoporiidae, Iniidae, and the recently extinct Lipotidae, as well as the true dolphins (Delphinidae), the porpoises (Phocoenidae) and the beluga and narwhal (Monodontidae) (Turvey et al. 2007; Marx et al. 2016).

In addition to the representatives of these extant families, the delphinidan fossil record includes the monogeneric families Albireonidae and Odobenocetopsidae, as well as a likely non-monophyletic group of more archaic taxa, of which many were formerly grouped in the clade Kentriodontidae (Muizon, 1988a; Muizon et al. 2002; Barnes 2008; Marx et al. 2016; Lambert et al. 2017, 2021; Peredo et al. 2018; Kimura & Hasegawa 2019). These disparately sized earliest delphinidans first appear in the fossil record in the upper Oligocene, but are predominantly known from the Miocene around the world (Ichishima et al. 1994; Dawson 1996; Marx et al. 2016). Since the erection of Kentriodontidae, several subfamilies had been recognized (Kampholophinae, Kentriodontinae, Lophocetinae and Pithanodelphininae) to better systematically group these taxa (Barnes 1978; Barnes 1985; Muizon 1988a). Lambert et al. (2017) however carried out the first phylogenetic analysis including more than a minimum of kentriodontid taxa, showing none of these kentriodontid subfamilies to be monophyletic. Hereafter, we provisionally refer to Kentriodontidae as the group defined by Lambert et al. (2021), retaining only *Kentriodon* and *Rudicetus* within this family. This definition of Kentriodontidae was supported by several subsequent phylogenetic analyses (e.g., Bianucci et al. 2022; Boessenecker & Geisler 2023). It should be noted however that the exact contents of Kentriodontidae remain debated (e.g. Peredo et al. 2018; Kimura & Hasegawa 2019; Guo & Kohno 2023). Other odontocetes formerly included in Kentriodontidae are hereafter referred to as 'early delphinidans', as the investigation of the phylogenetic relationships among them is outside the scope of this work.

From the North Atlantic region, multiple early delphinidans (including kentriodontids) are described from the odontocete-rich Miocene deposits of the Calvert Cliffs (Maryland) and other localities along the U.S. Atlantic Coastal Plain (Godfrey & Lambert 2023). These include among others the type specimens of *Kentriodon pernix* Kellogg, 1927 and *Brevirostrodelphis dividum* (True, 1912), as well as a specimen of *Pithanodelphis cornutus* (du Bus, 1872) (Godfrey & Lambert 2023). The latter was originally described from the North Sea Basin, from where three other early delphinidans were also described based on cranial material. These include *Kentriodon hoepfneri* Kazár & Hampe, 2014 from the Middle/Upper Miocene of Groß Pampau (northern Germany), the cranially malformed specimen *Kentriodon* cf. *Kentriodon pernix* IRSNB M.2340 from the lower Middle Miocene of Antwerp (northern Belgium), and historical specimen IRSNB M.372, also originating from the Antwerp area, from most likely Lower to Middle Miocene strata (du Bus 1872; Misonne 1958; Kazár & Hampe 2014; Lambert et al. 2025). IRSNB M.372 was originally described by du Bus (1872) based on fragmentary cranial material and identified as *Phocaenopsis scheynensis* du Bus, 1872. Abel (1905) later redescribed the specimen and identified it as *Acrodelphis scheynensis*. Since the erection of the genus *Kentriodon* by Kellogg (1927) however, multiple authors have commented on the high similarity of this specimen to specimens referred to this genus, implying the need for a taxonomic revision of this specimen (Fordyce & Muizon 2001; Kazár & Hampe 2014). Other, more fragmentary early delphinidan records from the Antwerp area are described by Louwye et al. (2010) and Everaert et al. (2019), including two isolated teeth, two tympanic bullae and a right periotic from the Antwerpen and Kiel members of the Berchem Formation.

In the early 2000s, two fragmentary early delphinidan crania (specimens IRSNB M.2342 and IRSNB M.2343) were collected from lower Middle Miocene strata of the Antwerpen Member (Berchem Formation, Fig. 1D), during the excavation of a series of construction pits in Berchem, Antwerp (northern Belgium, Fig. 1B & C). Here we describe these two specimens and consider their systematic affinities within Delphinida. Additionally, we redescribe the historical specimen IRSNB M.372 and reassess its taxonomic status. Finally, we discuss the palaeobiogeographic and palaeoecological implications resulting from our systematic attributions.

Geological background

The Lower to Middle Miocene deposits of the Antwerp area (northern Belgium, Fig. 1B) are lithostratigraphically grouped in the Berchem Formation, which is formally described as a highly glauconiferous, fine to medium fine grained, green to blackish sand unit (De Meuter & Laga 1976; Louwye et al. 2020). These sediments were deposited in a shallow marine environment, at the southern margin of the North Sea Basin (Louwye et al. 2000; Fig. 1A). The Berchem Formation in the Antwerp area is further subdivided, from lower to higher in the stratigraphy, into the Edegem Member (mid-Burdigalian), the Kiel Member (mid- to upper Burdigalian) and the Antwerpen Member (Langhian to mid-Serravallian) (De Meuter & Laga 1976; Louwye et al. 2020). The Antwerpen Member can often be distinguished in outcrops from the underlying Kiel Member by its noticeably darker colour (e.g., Everaert et al. 2020, 2024; Deckers & Everaert 2022; Fig. 1D). Within the Antwerpen Member several characteristic layers have been identified by Deckers & Everaert (2022), which can be traced throughout the Antwerp area. These include, from lower to higher in the succession, the '*Haustator eryna* phosphatic horizon' and the '*Glycymeris* crag' shell bed (termed respectively layers S2 and S3 by them). The former was recently renamed the '*Ptychidia eryna*' phosphatic horizon (Everaert et al. 2024). Specimen IRNSB M.2342 was collected from just below the '*Glycymeris* crag' shell bed, and specimen IRSNB M.2343 from the *Ptychidia eryna* phosphatic horizon (Fig. 1D).

Materials & methods

Institutional abbreviations

CMM, Calvert Marine Museum, Maryland, U.S.A; IRSNB, Institut royal des Sciences naturelles de Belgique, Brussels, Belgium; LACM, Natural History Museum of Los Angeles County, California, U.S.A; MCAF, Museo Civico Archeologico di Feltre, Feltre, Italy; MNHN, Muséum national d'Histoire naturelle, Paris, France; USNM, National Museum of Natural History, Smithsonian Institution, Washington D.C., U.S.A.

Anatomical descriptions and comparisons

Specimens IRSNB M.2342, IRSNB M.2343 and IRSNB M.372 all consist of fragmentary cranial material curated in the palaeontology collection of the IRSNB. Specimens IRSNB M.2342 and IRSNB M.2343 were both found in the early 2000s by one of the authors (MB), who also mechanically prepared and reassembled these specimens. Specimen IRSNB M.372 was retrieved probably by military personnel during the early 1860s in an unknown locality of the area of Antwerp, and was subsequently reconstructed at the IRSNB.

The anatomical terminology herein follows primarily that of Mead & Fordyce (2009). The crania were photographed using a Canon EOS 90D digital camera and a stabilizer. Digital images were processed in Adobe Photoshop and anatomical plates were drawn in Adobe Illustrator. Cranial elements were measured using a caliper (0.1 mm precision).

Comparisons with other early delphinidans were primarily done using the available literature, photos from past visits to other collections (CMM, MNHN, USNM), high-quality casts of crania (*Kentriodon pernix* USNM 10670, *Brevirostrodelphis dividum* USNM 7278, and *Lophocetus repenningi* Barnes, 1978 USNM 23886) and the type specimens of *Tagicetus joneti* Lambert et al., 2005 IRSNB M.1892 and *Pithanodelphis cornutus* IRSNB M.373.

Biostratigraphical analysis

About 20 grams of sediment associated with specimen IRSNB M.2342, was macerated for a biostratigraphical analysis based on dinoflagellate cysts. The maceration method followed Louwye et al. (2000). The sample held a well-preserved and diverse dinoflagellate cyst assemblage. A total of 250 specimens were counted in non-overlapping traverses under transmitted light at 200x magnification using a Zeiss Axio Imager A2 microscope.

Systematic palaeontology

Order **Cetacea** Brisson, 1762
Clade **Neoceti** Fordyce & Muizon, 2001
Suborder **Odontoceti** Flower, 1867
Infraorder **Delphinida** Muizon, 1984
Genus *Brevirostrodelphis* Godfrey & Lambert, 2023

Brevirostrodelphis aff. *B. dividum*

Figs. 2-5, Tab. 1

Referred specimen: IRSNB M.2342, a fragmentary cranium with a largely preserved facial region.

Locality: IRSNB M.2342 originates from a former construction pit in Berchem, Antwerp (northern Belgium, Fig. 1B & C). The general geographic coordinates of the discovery locality are: 51° 11' 25,7" N, 4° 26' 19,8" E.

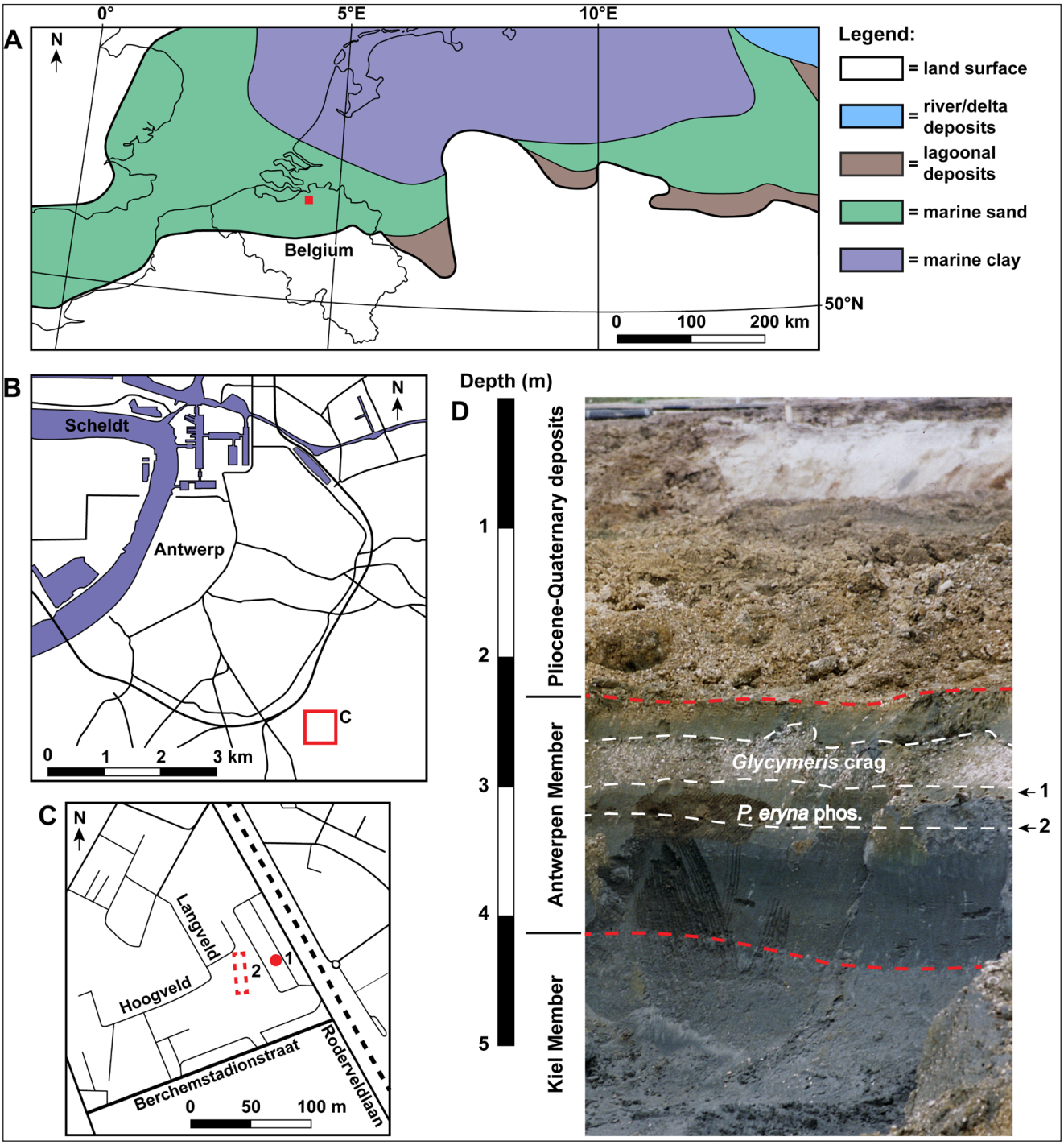

Fig. 1 - Geographic situation and general lithostratigraphic section of the discovery locality of *Brevirostrodelphis* aff. *B. dividum* IRSNB M.2342 and *Brevirostrodelphis* sp. IRSNB M.2343. A) Paleogeographic reconstruction of the southern North Sea Basin during the late Langhian (Middle Miocene), modified from Knox et al. (2010) and Gibbard & Lewin (2016). The present location of Antwerp city is indicated by a red square. B) General overview of Antwerp city with the discovery locality indicated by a red square. Black lines indicate main national roads and highways. C) Detailed map of the discovery locality with the finding locations indicated by a red dot (IRSNB M.2342) and a dashed red square (IRSNB M.2343). Full black lines indicate roads; the dashed black line indicates a railroad. D) General lithostratigraphic section of the discovery locality. The red dashed lines graphically delineate the main lithostratigraphic units (note that the Pliocene and Quaternary deposits are not graphically differentiated here, but grouped together as 'Pliocene-Quaternary deposits'). '*Glycymeris* crag' and '*P. eryna* phos.' indicate respectively the '*Glycymeris* crag' storm deposit (delineated by two white, dashed lines) and the '*Ptychidia eryna* phosphatic horizon' (marked by a single white, dashed line). '1' and '2' indicate the stratigraphic levels of specimens IRSNB M.2342 and IRSNB M.2343, respectively.

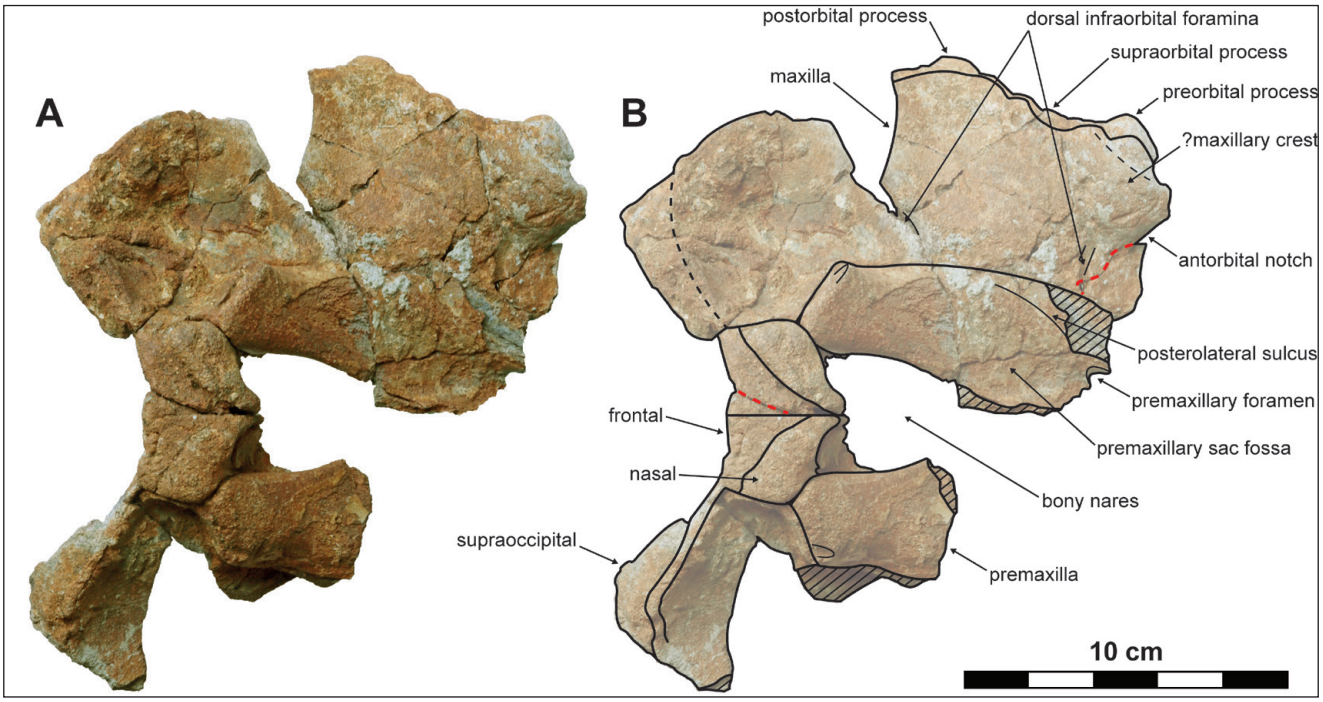

Fig. 2 - Dorsal view of the partial cranium of *Brevirostrodelphis* aff. *B. dividum* IRSNB M.2342. A) Dorsal view, photograph, and B) corresponding interpretative line drawing. Parallel lines indicate areas of breakage and red dashed lines indicate fractures. The black dashed lines indicate the lateral margin of the suggested maxillary crest (right, indicated) and the left side of the nuchal crest (left) being obscured by indurated sediment.

Horizon and age: IRSNB M.2342 was collected in-situ from just below the characteristic '*Glycymeris* crag' shell bed (Fig. 1D) of the Antwerpen Member (Berchem Formation) (see 'Geological background' for more details). The biostratigraphical analysis with dinoflagellate cysts of the sediment associated with skull IRSNB M.2342 indicated the presence of the marker species *Labyrinthodinium truncatum truncatum*, a species with a lowest occurrence located at the Burdigalian – Langhian boundary. The species defines the lower boundary of the *Labyrinthodinium truncatum* biozone (Dybkjær & Piasecki 2010). The marker species *Unipontedinium aquaeductum* of the superjacent eponymous biozone was not recorded. The sediment sample thus belongs to the Langhian *L. truncatum* biozone (15.97 Ma. to 14.8 Ma.) (Dybkjær & Piasecki 2010). An early Langhian age is subsequently assigned to IRSNB M.2342.

Description

General state of preservation. The cranium is fragmentarily preserved, with the rostrum, right orbit, basicranium and exoccipitals missing, and the parietals and supraoccipital almost completely missing. An uninformative detached fragment of the presphenoid with part of the vomer is preserved, but not described nor illustrated herein.

Premaxilla. The rostral portions of the premaxillae are completely missing, with only the posterior parts of the left and right premaxilla being preserved for 11 cm and 6.1 cm respectively. The premaxillae as preserved are symmetrical. The posterior part of the left premaxillary foramen is preserved and is situated just posterior to the level of the antorbital notch. The posterolateral sulcus is shallow and its posterior extent is unclear due to the poor preservation of the premaxillae in that area. Anterior to the bony nares, the premaxillary sac fossa forms a pronounced transverse concavity in the medial part of the premaxilla (Fig. 4). The medial margin of the premaxilla strongly rises dorsally in this region, making an erect, thin edge along the medial exposure of the maxilla. Lateral to the anterior part of the bony nares, the premaxillary sac fossa is only slightly transversely concave. It can be inferred that the bony naris would have been anteriorly closed by the medial margin of the premaxilla together with the medially located dorsal exposure of the maxilla. The medial margins of the premaxillae along the bony nares are gradually concave in dorsal view, resulting in the bony nares being anteriorly elongate. The lateral margin of the nasal portion of the premaxilla is evenly and gradually convex. The posterolateral margin of the premaxilla along the raised medial edge of the maxilla is straight and directed anterolaterally. This region is not anteroposteriorly thickened, but the lateral end of this margin projects shortly dorsal to the maxilla (Fig. 3). Each premaxilla is posterolaterally bounded

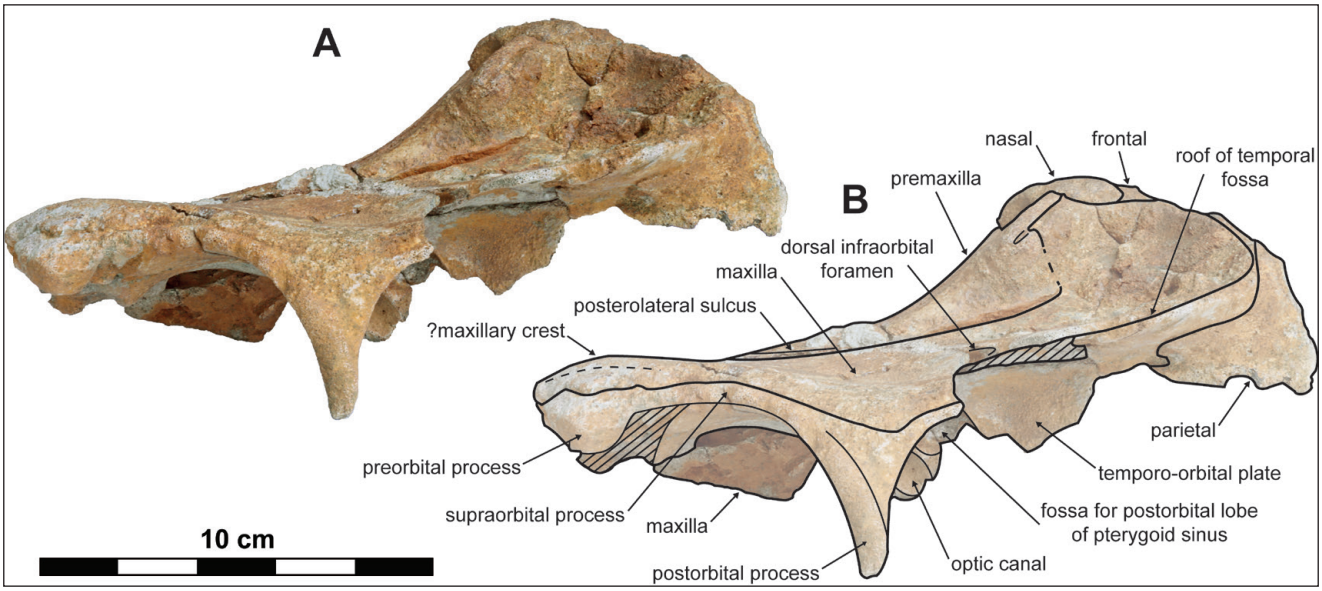

Fig. 3 - Left lateral view of the partial cranium of *Brevirostrodelphis* aff. *B. dividum* IRSNB M.2342. A) Left lateral view, photograph, and B) corresponding interpretative line drawing. Parallel lines indicate areas of breakage. The dashed lines indicate the lateral margin of the suggested maxillary crest (left, indicated) and the premaxilla-maxilla suture (right) being partly obscured by indurated sediment.

by the maxilla and posteromedially contacts the lateral part of the anterior face of the nasal, not reaching the dorsal exposure of the corresponding frontal. In lateral view the posterior margin of the premaxilla dorsally almost reaches the same elevation as the dorsal face of the nasals and frontals on the skull vertex.

Maxilla. The rostral portions of the maxillae are completely missing. The left maxilla is largely preserved in the facial region of the skull, except for a broken fragment of its posterolateral part above the temporal fossa and at the moderately abraded lateral part of the left orbit. Only the posteriormost part of the right maxilla is preserved. Of the left antorbital notch only the lateral wall is preserved. However, based on this preserved part it can be proposed that the antorbital notch would have been widely anterolaterally open. In the region of the antorbital process, remnants of a low, anteromedially oriented maxillary crest with a concave anterolateral margin can tentatively be recognized, though the degree of abrasion for this region made of more spongy bone is difficult to estimate. Posteromedial to this low crest, the dorsal surface of the maxilla is flat. Towards the posterior part of the supraorbital process, and in the postorbital region, the dorsal surface of the maxilla is slightly depressed in its lateral part (Fig. 3). Near its posterior and posteromedial margin, the maxilla abruptly rises dorsally, resulting in the maxilla being oriented vertically at the contact with the lateral side of the skull vertex and almost vertically at its posterior margin. In dorsal view, the posterior margin of the maxilla is oriented posterolaterally. The posterolateral margin of the maxilla is evenly convex in dorsal view and turns anterolaterally. A dorsal infraorbital foramen is present just lateral to the left premaxilla-maxilla suture and slightly posterior to the level of the premaxillary foramen (Fig. 2); it opens laterally with a diameter of 4.5 mm. The sulcus extending posterolaterally from a second dorsal infraorbital foramen is visible posterior to the level of the postorbital process, but the exact location of the foramen is unknown due to breakage of the dorsal surface of the maxilla in this region. The maxillae are overall relatively wide and flat in dorsal view in the facial region, resulting in an overall wide and low appearance of this region of the skull.

Frontal. In dorsal view, the left frontal is largely preserved in the orbit region, but its lateral margin is abraded in the pre- and supraorbital region together with the associated maxilla. The dorsal exposure of the frontals at the skull vertex is well preserved, but the left side of the vertex (including the left frontal and nasal) is slightly displaced anteriorly due to a longitudinal fracture (Fig. 2). In ventral view, the left frontal is largely preserved, except for its abraded part in the preorbital region and a broken fragment

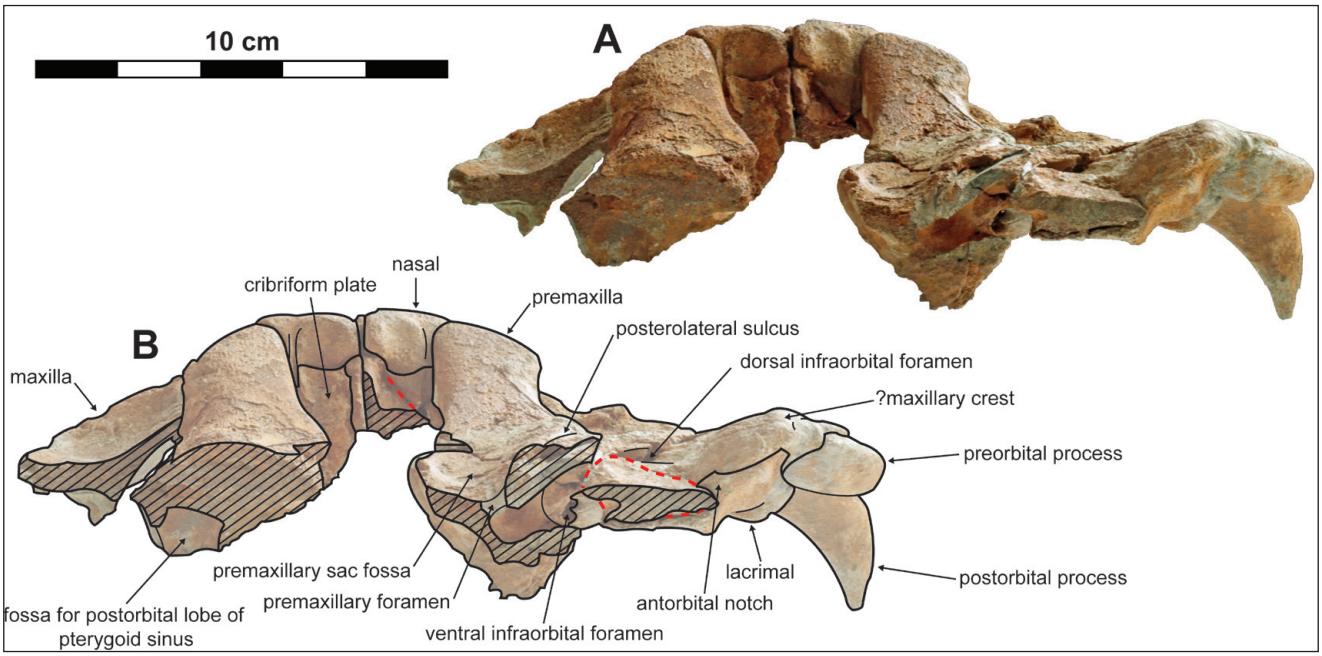

Fig. 4 - Anterior view of the partial cranium of *Brevirostrodelphis* aff. *B. dividum* IRSNB M.2342. A) Anterior view, photograph, and B) corresponding interpretative line drawing. Parallel lines indicate areas of breakage and red dashed lines indicate fractures. The black dashed line indicates the lateral margin of the suggested maxillary crest.

above the temporal fossa. While the dorsal exposure of the frontal in the pre- and supraorbital regions is unclear due to local abrasion, the postorbital process is narrowly dorsally exposed. In lateral view the postorbital process is relatively long ventrally, making a narrow, ventrally pointing triangle. An anteroposteriorly rounded ridge is present along the anterolateral margin of the postorbital process (Fig. 3). Together with the nasals, the dorsalmost exposure of the frontals forms the skull vertex, which has an overall wide pentagonal outline and is relatively low and tabular. The dorsal exposures of the frontals on the skull vertex are symmetrical and subtriangular in outline, making a deep (about 16 mm) and broad wedge between the nasals. The frontals are markedly transversely narrower than nasals on the vertex. The interfrontal suture on the vertex is straight and directed anteroposteriorly. The combined posterior margin of the frontals on the skull vertex is slightly anteriorly concave. The lateral faces of the frontals on the vertex are straight and laterally contact the maxilla for a short distance (less than 4 mm on the right side). The dorsal face of the frontals on the vertex is tabular and slightly lower than the dorsalmost surface of the nasals. Best seen on the right side of the nuchal crest, the frontal is exposed as a narrow stripe (maximum width = 4 mm) between the maxilla and supraoccipital. In ventral view, a deep fossa for the postorbital lobe of the pterygoid sinus is located just posterior to the optic canal and infratemporal crest. The latter is only partly preserved due to local abrasion, this process remaining relatively low until the base of the postorbital process.

Nasal. Both nasals are well preserved on the skull vertex. They are symmetrical, subtriangular and anteromedially elongated in their dorsal outline. The internasal suture is relatively short (15 mm), straight and is oriented anteroposteriorly. The anteromedial tip of the joined nasals extends anteriorly between the bony nares for about 4 mm. On the anterior face of the nasal, a narrow, shallow and vertically oriented groove is present, just medial to the nasal-premaxilla suture (Fig. 4). This groove flares dorsally, resulting in a depression on the anterodorsal face of the nasal. The dorsal surface of the nasal rounds over anteroposteriorly and slightly descends anteromedially to form a shallow and narrow internasal fossa (Figs. 3 & 4).

Lacrimal and jugal. The left lacrimal is largely preserved on the ventral side of the skull, with only its anterolateralmost part missing. On the ventral surface of the lacrimal, the lacrimomaxillary fossa is present as a prominent, broad (11 mm at midlength), and anterolaterally oriented groove which terminates posteromedially into the ventral infra-

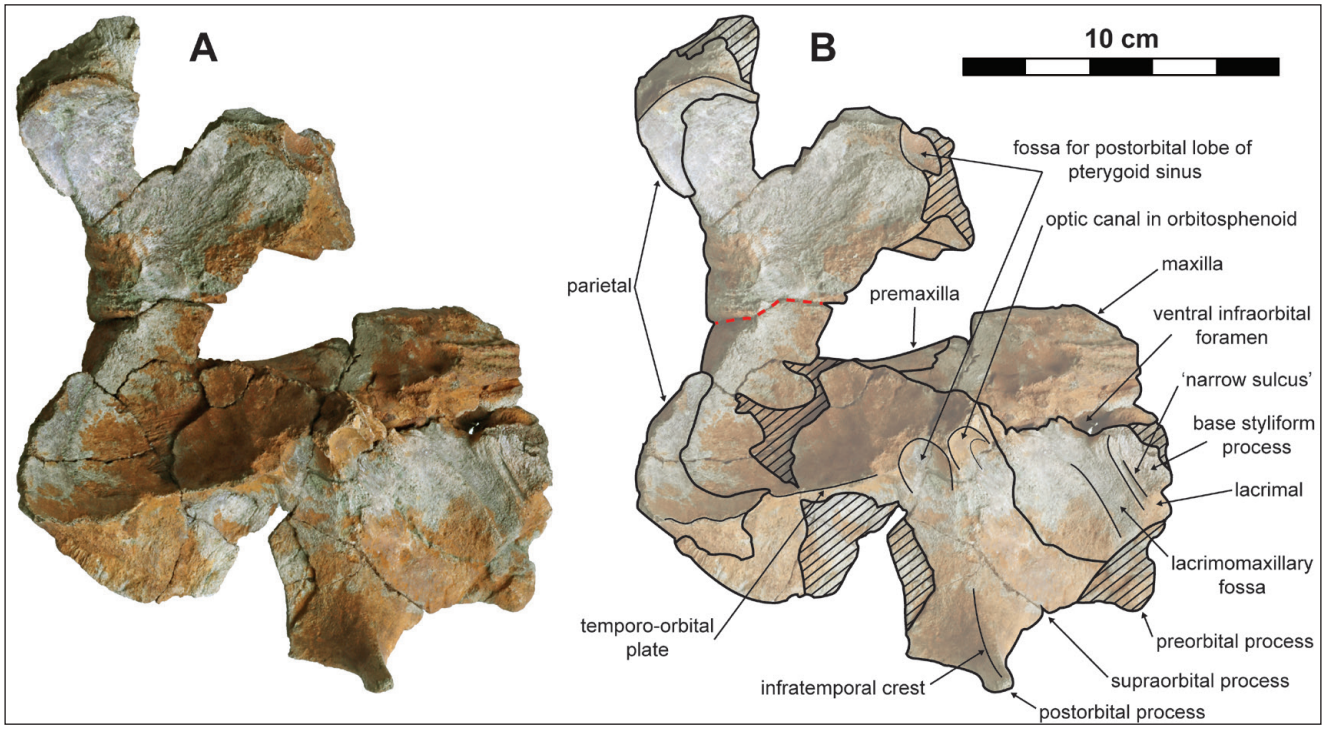

Fig. 5 - Ventral view of the partial cranium of *Brevirostrodelphis* aff. *B. dividum* IRSNB M.2342. A) Ventral view, photograph, and B) corresponding interpretative line drawing. Parallel lines indicate areas of breakage and red dashed line indicates fractures.

orbital foramen. The ventral infraorbital foramen is ovoid, anterolaterally elongated and opens posteroventrally. The lacrimal-frontal suture as preserved on the ventral surface of the skull is posterolaterally convex. Located just posterior to the antorbital notch, the base of the styliform process of the jugal is separated from the lacrimomaxillary fossa by a narrow sulcus, which is parallel to the long axis of the latter (Fig. 5). No indication of a suture between the lacrimal and jugal could be found there, suggesting that the two bones were at least partly fused.

Orbitosphenoid. Though suture lines are difficult to follow in that region, the left orbitosphenoid is at least partly preserved posterior to the fossa for the postorbital lobe of the pterygoid sinus (Fig. 5). It is excavated by the optic canal, leading posteromedially to the slit-like optic foramen. The latter appears to have been separated from the inferior and superior orbital fissures.

Parietal. Each parietal is partly preserved in the posterodorsal region of the corresponding temporal fossa. The parietal sends a mediodorsal projection towards the vertex of the cranium, best seen in ventral view of the open endocranial cavity (Fig. 5). On the left side the incomplete parietal reaches medially a level that is 20 mm distant from the sagittal plane.

Supraoccipital. The preserved outline of the posterior margin of the frontals indicates that the anterior margin of the supraoccipital was anteriorly convex (Fig. 2).

Ontogeny and size estimation

In absence of the postcranial skeleton, basicranium, and rostrum, the ontogenetic stage of IRSNB M.2342 is here assessed based on the degree of fusion of the preserved dorsal cranial sutures. This region has been shown to provide clues on the degree of physical maturity in multiple extant delphinidans, albeit displaying species-specific patterns (e.g., Mead & Potter 1990; Calzada et al. 1997; Chen et al. 2011). The degree of closure for cranial sutures, with some sutures remaining partly open (e.g. maxilla-premaxilla, supraoccipital-frontal, and parietal-frontal sutures) and others being roughly closed (e.g. frontal-maxilla sutures) suggests that IRSNB M.2342 corresponds to a young individual, possibly not physically mature, but potentially somewhat older than the holotype of *Brevirostrodelphis dividum*. Indeed, the latter displays for example more conspicuously open sutures between the maxillae and frontals along the nuchal crest.

The greatest skull width of IRSNB M.2342 is estimated to be ca. 226 mm at the level of the postorbital process. Employing this measurement as a substitute for the bizygomatic width, the total body length of IRSNB M.2342 is estimated at 1,86 m, using the equation provided by Pyenson & Sponberg (2011) for stem delphinoids. This body size estimation is comparable to that of adults of the extant dusky dolphin (*Lagenorhynchus obscurus* (Gray, 1828)) (Van Waerebeek & Würsig 2017). Using the same equation, the total body length of the holotype of *B. dividum* (bizygomatic width = 163 mm (True 1912)) is estimated at 1,38 m. The estimation for IRSNB M.2342 remains however tentative due to the fragmentary preservation of this specimen, preventing an accurate measurement of the bizygomatic width.

Comparison and discussion

Following the remarks by Nobile et al. (2024) on *Kentriodon hoepfneri* and *K. obscurus* Kellogg, 1931 LACM 21256, we include these specimens in our comparisons, but hereafter refer to them as '*K. hoepfneri'* and *K.* '*obscurus*'. IRSNB M.2342 is herein not compared to *Belonodelphis peruanus* Muizon, 1988, *Herbeinodelphis nancei* Godfrey & Lambert, 2023 and *Incacetus broggii* Colbert, 1944, as the holotypes of these species lack preserved areas that overlap with the specimen described herein, and can thus not be compared with the latter.

IRSNB M.2342 can be identified as a delphinidan due to the width of its frontals not exceeding that of the nasals on the skull vertex (Muizon 1988a). Within Delphinida it differs from Lipotidae in lacking elevated frontals on the skull vertex; from Iniidae in lacking a frontal boss on the skull vertex; from Pontoporiidae in lacking anteroposteriorly long and narrow nasals; from Monodontidae in lacking a dorsal exposure of the maxilla medially to the premaxilla along the bony nares; from Phocoenidae in lacking premaxillary eminences anterior to the bony nares and in lacking a frontal boss on the skull vertex; from Delphinidae in possessing posteriorly symmetrical premaxillae; from Albireonidae in lacking premaxillary eminences anterior to the bony nares; and from Odobenocetopsidae in its posteriorly located bony nares (Muizon 1988a, 1993; Barnes 2008; Colpaert 2015; Marx et al. 2016).

Among Miocene early delphinidans, it differs from *Cammackacetus hazenorum* Godfrey & Lambert, 2023*, Hadrodelphis calvertense* Kellogg, 1966*, Macrokentriodon morani* Dawson, 1996 and *Miminiacetus pappus* (Kellogg, 1955) in its markedly smaller skull size; from *Kampholophos serrulus* Rensberger, 1969 and *Rudicetus squalodontoides* (Capellini, 1878) in its conspicuously posterolaterally more expanded maxilla; from *Atocetus* spp., *H. calvertense*, *Lophocetus* spp., *Mi. pappus, Pictodelphis kidwellae* Godfrey & Lambert, 2023, *Pithanodelphis cornutus*, *Platysvercus ugonis* Guo & Kohno, 2023 and *Sarmatodelphis moldavicus* Kirpichnikov, 1954 in lacking a marked lateral constriction on the skull vertex; from *Atocetus* spp.*, Lophocetus* spp.*, Mi. pappus, Pic. kidwellae, Pit. cornutus, Sa. moldavicus, Sophianaecetus commenticius* (Kazár, 2005)*, Westmorelandelphis tacheroni* Godfrey & Lambert, 2023 and *Wimahl chinookensis* Peredo et al., 2018 in its tabular skull vertex; from *C. hazenorum* and *H. calvertense* in the width of its frontals not exceeding that of the nasals on the skull vertex; from *K. serrulus*, *R. squalodontoides*, *Tagicetus joneti* and *We. tacheroni* in its anteromedially elongated, subtriangular nasals; from *C. hazenorum, Ma. morani, Pit. cornutus, So. commenticius, T. joneti* and *We. tacheroni* in lacking a vertical notch on the anterior face of the nasal; and from *Atocetus* spp. and *Wi. chinookensis* in its proportionally much smaller nasals. It further differs from *Pl. ugonis* in the nasals being laterally bounded by the maxillae.

Among the members of the species-rich genus *Kentriodon,* IRSNB M.2342 differs from *K. hobetsu* Ichishima, 1994, *K. 'obscurus'* and *K. pernix* in its markedly larger skull size; from *K. diusinus* Salinas-Márquez et al., 2014*, K. hobetsu, K. 'obscurus' and K. pernix* in its distinctly proportionally wider skull; from '*K. hoepfneri'* and *K. pernix* in its subtriangular nasals and lacking a vertical notch on the anterior face of the nasal; and from *K. sugawarai* Guo & Kohno, 2021 in its nasal posteriorly not reaching the supraoccipital. It further differs from *K. diusinus* in its nasals laterally contacting the maxillae. IRSNB M.2342 shows some similarity to *K. nakajimai* Kimura & Hasegawa, 2019 at the level of the skull vertex, but clearly differs from this species in e.g. lacking a vertical notch on the anterolateral face of its nasal; its longer postorbital process; and in lacking a greatly enlarged fossa for the preorbital lobe of the pterygoid sinus.

IRSNB M.2342 also shows some similarity to *Kentriodon schneideri* Whitmore & Kaltenbach, 2008, most notably in their similar overall skull size and

Dimension	*Brevirostrodelphis* aff. *B. dividum* (IRSNB M.2342)	*Brevirostrodelphis dividum* (USNM 7278)	*Kentriodon schneideri* (USNM 323772)
Width of left premaxilla at preorbital process	e37	31	-
Width of left maxilla at preorbital process	+50	37.5	-
Dorsoventral length of preorbital process of frontal	11	9	-
Combined thickness of frontal + maxilla, at lateral margin of preorbital process of frontal	16	13.5	-
Width of left maxilla at mid-length orbit	+50	34	-
Width of left premaxilla at mid-length orbit	e40.5	39.5	-
Maximal dorsoventral thickness of frontal + maxilla, at mid-length orbit	10	3	-
Skull width at maximum lateral extent of supraorbital process	e188	157	e170
Transverse width of left premaxilla at postorbital process	34	35.5	-
Transverse width of maxilla at postorbital process	59	33.5	-
Dorsoventral length of postorbital process	29	*29	-
Length of orbit (anteroposterior distance between ventral tip of postorbital process and ventral tip of preorbital process)	53	48.5	-
Width of bony nares at anterior margin nasal	34.5	32.5	-
Width of bony nares at level of postorbital process	26	21.5	-
Anteroposterior length of right nasal	27	18	-
Transverse width of right nasal	23.5	20.5	-
Anteroposterior length of right frontal on skull vertex	21	27	-
Transverse width of right frontal on skull vertex	21	17	-
Length of vertex (measured from posteriormost margin of frontal to anteriormost margin of nasal, along the sagittal plane)	30	35.5	e30
Width of vertex (maximal distance between medial margins of maxillae at the skull vertex)	50	39.5	49

Tab. 1 - Measurements (in mm) for *Brevirostrodelphis* aff. *B. dividum* IRSNB M.2342, *Brevirostrodelphis dividum* USNM 7278 (holotype) and *Kentriodon schneideri* USNM 323772 (holotype). '+' indicates a minimal value, 'e' indicates an estimate value and '-' indicates non-available data. '*' indicates measurements taken from True (1912). Other measurements for *B. dividum* USNM 7278 are taken on a cast of this specimen housed at the IRSNB. Measurements for *K. schneideri* USNM 323772 are taken from Whitmore & Kaltenbach (2008).

cranial proportions, and the almost identical proportions of their tabular skull vertices (Tab. 1). IRSNB M.2342 differs however from *K. schneideri* in e.g. the more anteriorly positioned orbit (the postorbital process of IRSNB M.2342 being in line with the anterior edge of the bony nares, instead of mid-length of the bony nares as in *K. schneideri*); the less strongly dorsally convex lateral margin of its orbit; and the less steeply posteriorly ascending nasal portion of the premaxilla. More detailed comparison between IRSNB M.2342 and the holotype of *K. schneideri* (USNM 323772) is however largely inhibited by the preservational state of the facial region of the latter. USNM 323772 shows for instance incompletely preserved orbits, invisible nasal-frontal sutures on the skull vertex, and abraded anterior faces of the nasals and dorsal surface of the nasal portion of the premaxillae. All of this impedes a more in-depth comparison of these features between both specimens. *K. schneideri* USNM 323772 was collected from the Pungo River Formation, which has approximately an Aquitanian to Langhian age and thus potentially overlaps with IRSNB M.2342 in its stratigraphic age (Ward 2008; Whitmore & Kaltenbach 2008).

IRSNB M.2342 shows much similarity to *Brevirostrodelphis dividum* in the overall low and wide appearance of the facial region of its skull and, most importantly, the highly similar facial morphology. It displays for instance a wide and medially concave premaxillary sac fossa almost identical in shape to USNM 7278 (holotype of *B. dividum*); a prominent and anterolaterally oriented lacrimomaxillary fossa; a ventrally long postorbital process (also possessing an anteroposteriorly rounded ridge); straight and anterolaterally directed posterolateral margins of the premaxillae; and a wide, pentagonal and tabular skull vertex. It differs however from USNM 7278 in the proportionally wider maxillae and subsequently wider facial region of its skull (Tab. 1); the more massive maxilla and frontal in lateral view of the orbital region (Tab. 1); the more dorsally raised nasal process of its premaxilla; and the lacrimomaxillary fossa which terminates anteromedially into the ventral infraorbital foramen. On the skull vertex, the frontals of IRSNB M.2342 differ in being subtriangular in outline with a posteriorly convex nasal-frontal suture. The nasals of IRSNB M.2342 also differ in lacking an inflated anterolateral process, their internasal suture being shorter (resulting in

their subtriangular outline) and their anteromedial tip being sharper.

Some of the variation between IRSNB M.2342 and USNM 7278 can however potentially be explained by their different ontogenetic age, as inferred by the higher degree of closure of the cranial sutures of IRSNB M.2342. Moreover, the postcranial skeleton of USNM 7278 displays free epiphyses for all retrieved vertebrae (6 cervicals, excluding the atlas which does not bear epiphyses, 9 thoracics, 6 lumbars and 5 caudals) and for the left humerus, and both thyrohyals being separate from the basihyal (True 1912). These observations point to a calve (see Perrin (1975) for the extant delphinid *Stenella attenuata* (Gray, 1846)), possibly less than one year old (see Galatius & Kinze (2003) for the extant phocoenid *Phocoena phocoena* (Linnaeus, 1758)). In *S. attenuata* for example, the postorbital process becomes more massive with ontogenetic development, potentially explaining the more massive postorbital process of IRSNB M.2342 compared to USNM 7278 (Perrin 1975). In the extant pontoporiid *Pontoporia blainvillei* (Gervais & d'Orbigny, 1844), the premaxillae are proportionally wider than the maxillae in immature specimens, possibly also explaining the proportionally wider maxilla relative to the premaxilla in IRSNB M.2342 compared to USNM 7278 (del Castillo et al. 2014). Some of the other differences between IRSNB M.2342 and USNM 7278 (e.g. the wider and more massive maxilla and frontal) could be envisaged to be a result of the older ontogenetic age of the former. Other differences (e.g. at the level of the skull vertex) are perhaps less clearly a result of this, but this hypothesis can at present not be ruled out. USNM 7278 was found in one of the lower lithostratigraphic zones of the Calvert Formation (Chesapeake Group) in Maryland (U.S.A.), thus presumably from the Fairhaven Member, which has a Burdigalian age (Kidwell et al. 2015). USNM 7278 is thus probably geologically older than IRSNB M.2342.

Considering its high morphological similarity to *B. dividum*, IRSNB M.2342 is here regarded to potentially represent an ontogenetically older specimen of *B. dividum,* or of a closely related species. Pending the discovery of more complete specimens conspecific to IRSNB M.2342 from the North Sea Basin, preferentially including the ear bones, and the publication of ontogenetically older specimens of *B. dividum* from the same stratigraphic horizon as the holotype along the US east coast, we provisionally identify IRSNB M.2342 as *Brevirostrodelphis* aff. *B. dividum*.

Brevirostrodelphis sp.

Figs. 6 & 7, Tab. 2

Referred specimen: IRSNB M.2343, a fragmentary cranium preserved in two parts.

Locality: IRSNB M.2343 originates from a former construction pit in Berchem, Antwerp (northern Belgium), in proximity to the discovery location of IRSNB M.2343 (Fig. 1C). The general geographic coordinates of the discovery locality are: 51° 11' 25,7" N, 4° 26' 19,8" E.

Horizon and age: IRSNB M.2343 was collected in-situ from the characteristic '*Ptychidia eryna* phosphatic horizon' (Fig. 1D) of the Antwerpen Member (Berchem Formation) (see 'geological background' section for more details). Louwye et al. (2000, 2010) and Everaert et al. (2020, 2024) dated this layer as early Langhian, based on their recognition of dinocyst biozone DN4 of de Verteuil & Norris (1996). Consequently, an early Langhian age is assigned here for IRSNB M.2343.

Description

General state of preservation. The cranium is fragmentarily preserved in two parts. The first part (Fig. 6) consists of the left orbit with its associated frontal, maxilla and the left lacrimal. The second part (Fig. 7) consists of the posterior parts of the right premaxilla, maxilla and frontal, the right nasal, part of the dorsal exposure of the right frontal on the skull vertex, the upper part of the right parietal in the temporal fossa, and a fragment of the supraoccipital.

Premaxilla. The posterior part of the right premaxilla is fragmentarily preserved for 8.1 cm. At the anteriormost preserved part of the premaxilla, the premaxillary sac fossa is only slightly transversely concave (Fig. 7E & F). At this level, just anterior to the bony naris, the medial margin of the premaxilla rises dorsally. At the level of the bony nares the dorsal surface of the premaxilla is transversely convex along its lateral portion and its lateral margin is laterally convex. The posterolateral sulcus is not recognized, possibly due to the fragmentary preservation of the premaxilla in that region, except for a short distance before the posterolateral corner of the premaxilla. The posterolateral margin of the premaxilla along the dorsally raised medial edge of the maxilla is straight, directed anterolaterally and forms a posterodorsolaterally oriented, rugose textured, flat dorsal surface. Below this flat surface, the posterior edge of the premaxilla is shortly an-

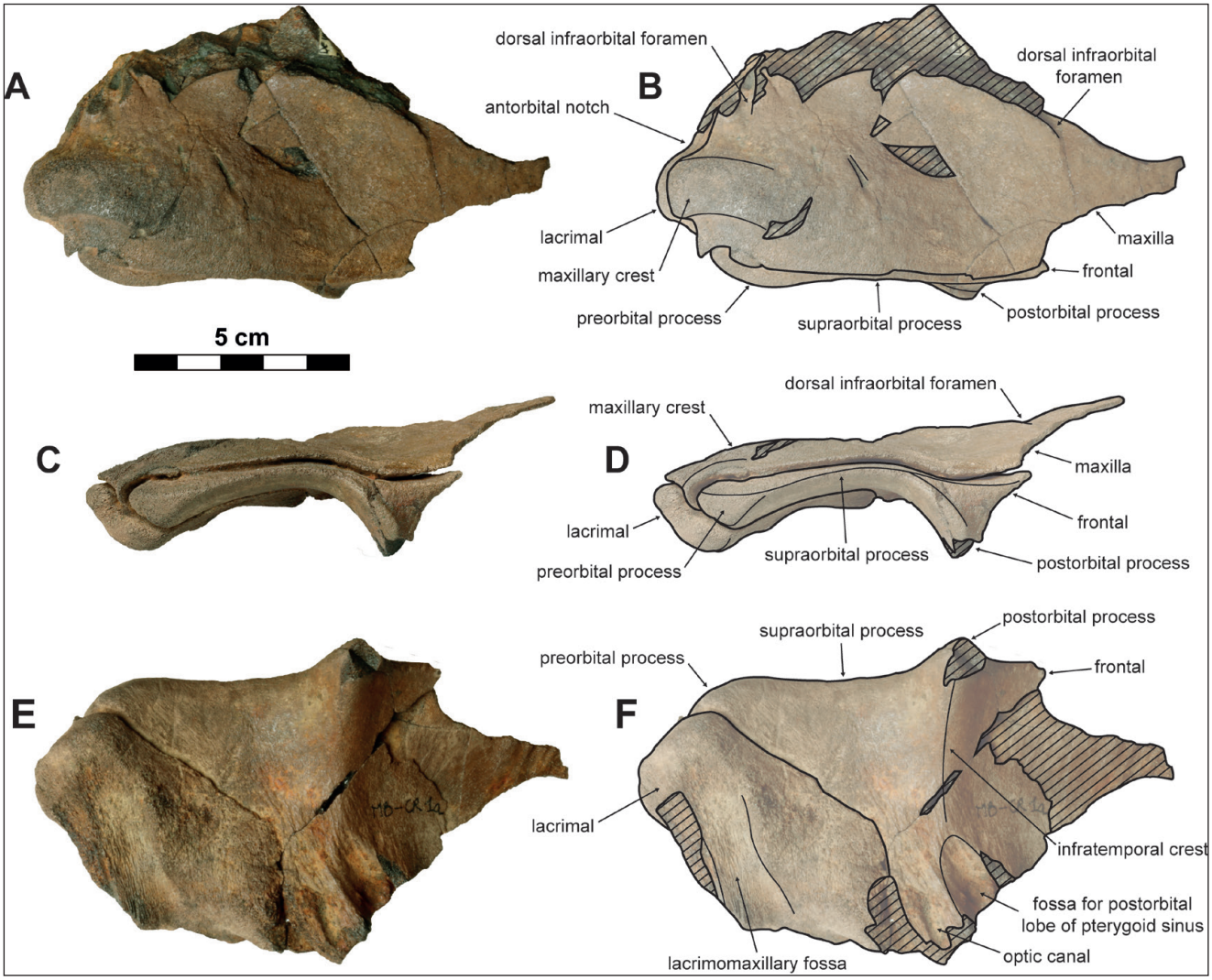

Fig. 6 - Dorsal, lateral and ventral views of the left orbit region of the fragmentary cranium of *Brevirostrodelphis* sp. IRSNB M.2343. A) Dorsal view, photograph, and B) corresponding interpretative line drawing. C) Lateral view, photograph, and D) corresponding interpretative line drawing. E) Ventral view, photograph, and F) corresponding interpretative line drawing. Parallel lines indicate areas of breakage.

terolaterally indented by the maxilla. The right premaxilla is posterolaterally bounded by the maxilla and posteromedially by the prism-like anterolateral process of the nasal. The posteriormost tip of the premaxilla dorsally almost reaches the same height as the dorsal face of the right nasal. The medial margin of the premaxilla in the area of the bony naris is evenly concave and oriented anteromedially.

Maxilla. In the left orbital region, a slightly anteromedially oriented, ca. 15 mm wide and dorsally flat maxillary crest is present on the left antorbital process. The lateral and medial margins of this maxillary crest are medially convex. In dorsal view, the lateral margin of the left maxilla is very slightly laterally convex in the orbital region. In lateral view the left maxilla gradually thickens from the level of the postorbital process towards the preorbital process. From the supra- to the antorbital region, the dorsal surface of the maxilla including the maxillary crest is dorsally convex in lateral view. The maxilla does not completely dorsally cover the frontal in the orbital region, leaving a narrow strip of dorsal exposure of the frontal in this region. At the level of the postorbital process, the dorsal surface of the left maxilla forms an anteromedially elongated, wide and shallow depression. Posterior to the postorbital process the maxilla only slightly rises posterodorsally in lateral view, resulting in the general low appearance of the skull in this region. On the left maxilla (Fig. 6), at about the level of the preorbital process, a laterally directed sulcus leaving from a partly preserved anterior dorsal infraorbital foramen is present, 7 mm medially to the maxillary crest. A second, partly preserved opening

to a dorsal infraorbital foramen is present on the left maxilla, just posterior to the level of the postorbital process and just medially to the level of the maxillary crest. This posterior dorsal infraorbital foramen on the left maxilla opens posterolaterally. At the anteriormost preserved part of the right maxilla (Fig. 7), a partly preserved dorsal infraorbital foramen is present, about just anterior to the level of the anterior part of the bony naris. Posteriorly, a second, partly preserved dorsal infraorbital foramen is present on the right maxilla, at the level of the posterior margin of the bony naris. This posterior dorsal infraorbital foramen on the right maxilla opens posterolaterally and corresponds to the right equivalent of the posterior dorsal infraorbital foramen on the left preserved maxilla, providing an approximate landmark to correlate both fragments of the skull. The dorsal surface of the right maxilla is slightly depressed in its posterolateralmost part, but medially forms a flattened, gently inclined surface in this region. At the contact with the skull vertex as preserved and the posterolateral margin of the premaxilla, the posteromedial margin of the maxilla abruptly rises dorsally, becoming almost vertically oriented. The posterior margin of the right maxilla along the nuchal crest is slightly posteriorly convex, almost straight, and oriented posterolaterally.

Frontal. The left frontal is almost completely preserved in the orbital region, except for the broken ventral tip of the postorbital process. The right frontal is partly preserved ventral and posterior to the right maxilla and on the skull vertex. In lateral view the preorbital process is triangular and moderately dorsoventrally thickened. The orbit roof is the highest just anterior to the postorbital process, from where it gently slopes down towards the preorbital process (Fig. 6C & D). In dorsal view the lateral margin of the supra- and preorbital process is oriented slightly anterolaterally, gradually increasing the dorsal exposure of the frontal in this region towards the preorbital process. In lateral view the postorbital process is oriented ventrally and appears to have originally formed a relatively elongated and narrow triangle. The postorbital process possesses a prominent, anteroposteriorly rounded ridge along the anterior margin of its lateral surface. Posterior and posterolateral to the right maxilla, the frontal is dorsally exposed for ca. 2 mm, preventing the maxilla from contacting the occipital shield. The anterolateral and lateral parts of the dorsal exposure of the right frontal on the skull vertex are broken for a large portion. Based on the outline of the underlying, preserved part of this bone, it can be inferred that the dorsal exposure of the right frontal on the skull vertex was originally rectangular in dorsal outline with the long axis oriented anteromedially and that it was narrower than the nasal. The preserved dorsal surface of the right frontal on the skull vertex has a rugose, pitted texture and gently slopes down medially. A knoblike protrusion of the right frontal extends for 2 mm anteriorly into the posterior margin of the nasal and is situated 6 mm laterally to the plane formed by the internasal suture, giving the nasal-frontal suture an angular aspect at this level. On the ventral surface of both frontals, the anteroposteriorly short but deep fossa for the postorbital lobe of the pterygoid sinus is situated just posterior to the infratemporal crest and posterolateral to the optic canal.

Nasal. In dorsal view, the general outline of the right nasal is rectangular with a long axis oriented anteromedially. The internasal suture is straight and oriented anteroposteriorly. An anteriorly protruding process is present on the lateral margin of the anterior face of the nasal. This anterolateral process of the right nasal tapers in width anteriorly and ventrally, forming a ventromedially elongated, prism-like structure along the lateral margin of the anterior face of the nasal. The anterolateral process does however not correspond to the presence of a well-defined vertical notch, as it does not laterally margin a pocket-like concavity on the anterior face of the nasal. The medial part of the anterior margin of the nasal is slightly anteriorly convex in dorsal view. A shallow depression is present on the anterodorsal face of the nasal, just medial to the anterolateral process of the nasal. The dorsal face of the nasal is slightly rounded anteroposteriorly and slopes medially, indicating the presence of a shallow and broad internasal fossa (Fig. 7E & F). Except for the knoblike anterior protrusion of the frontal described above, the nasal-frontal suture is straight and oriented anteromedially. Together with the dorsomedial exposure of the frontal, the dorsal face of the nasal forms the skull vertex, which can be inferred to have originally been wide pentagonal in its dorsal outline and tabular.

Lacrimojugal complex. The left lacrimal is largely preserved on the ventral side of the skull, but most (if not all) of the jugal lost. On the ventral side, the

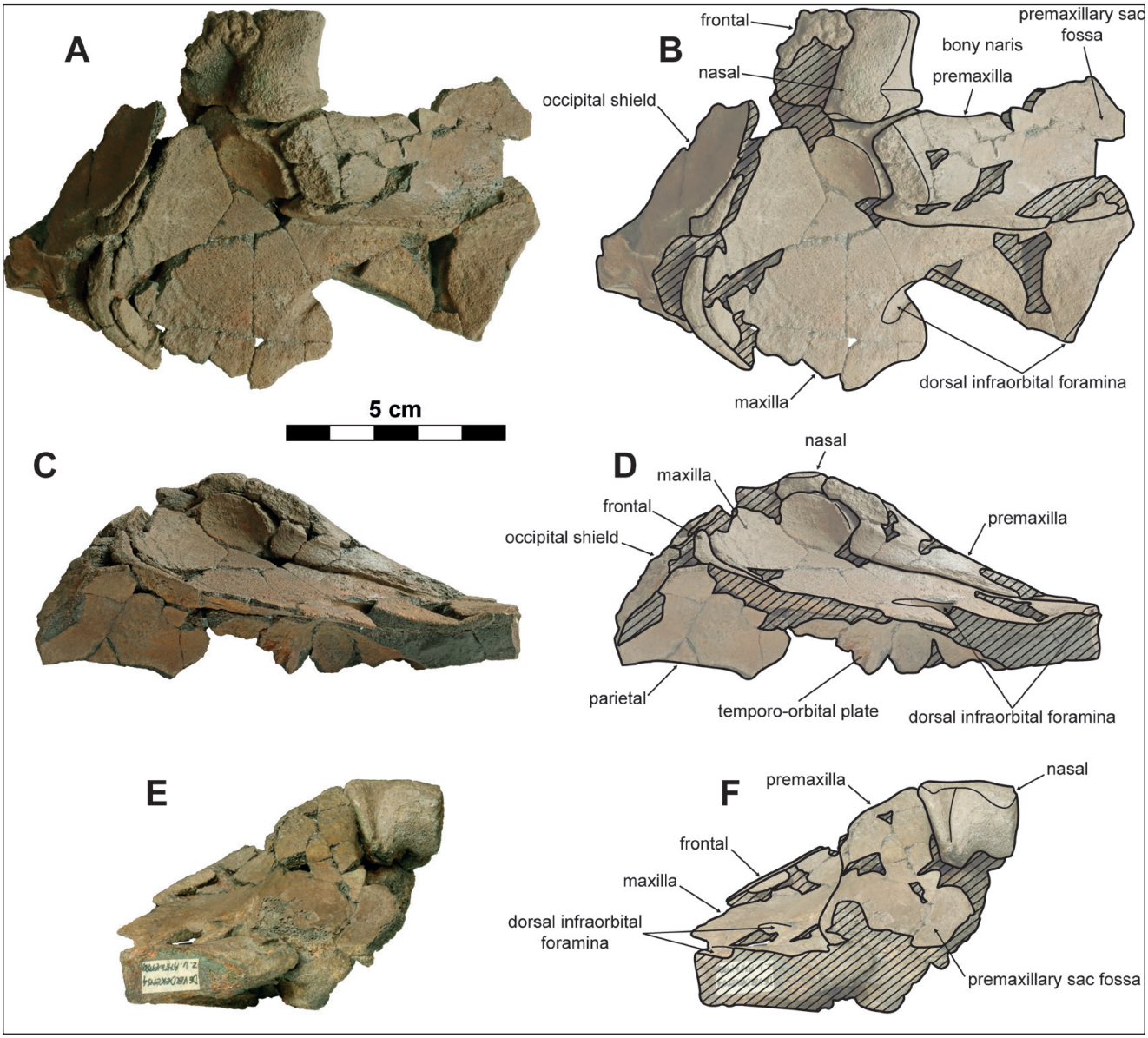

Fig. 7 - Dorsal, lateral and anterior views of the posterior fragment of the fragmentary cranium of *Brevirostrodelphis* sp. IRSNB M.2343. A) Dorsal view, photograph, and B) corresponding interpretative line drawing. C) Right lateral view, photograph, and D) corresponding interpretative line drawing. E) Anterior view, photograph, and F) corresponding interpretative line drawing. Parallel lines indicate areas of breakage.

lacrimomaxillary fossa is present as a wide (1,1 cm anteroposterior width) and anteroposteriorly concave groove which is oriented laterally and slightly anteriorly (Fig. 6E & F). The lacrimal-frontal suture is straight and oriented posteromedially in its anterior part, but abruptly turns medially past mid-length of the orbit. In lateral view, the lacrimal is exposed as a thick oblique plate directed anterodorsally from the ventralmost tip of the preorbital process to a short distance anterior to the anterior edge of the antorbital process of the maxilla. This plate thickens moderately posteroventrally and its ventral margin is ventrally convex, contributing to the ventrally bulging outline of the whole antorbital region. Together with the maxilla dorsally, the lacrimal forms the lateral wall of the antorbital notch, which is directed anterolaterally, making an angle of about 40-45° with the estimated sagittal plane of the skull.

Supraoccipital. The preserved right dorsolateral part of the occipital shield is transversely flat and slightly anteroposteriorly concave (Fig. 7A & B). The outline of the nuchal crest along the preserved part of the occipital shield suggests that this crest was originally anteriorly convex in dorsal view.

Parietal. The short portion of the parietal, preserved in the upper part of the right temporal

fossa (Fig. 7C & D), displays a dorsoventrally convex surface indicating at least some degree of lateral inflation for the endocranial cavity.

Ontogeny

The maturity of IRSNB M.2343 is assessed based on the degree of fusion of its cranial sutures (see section on ontogeny of IRSNB M.2342 for references). The degree of closure for cranial sutures, with most sutures remaining open (e.g. lacrimal-maxilla, lacrimal-frontal, frontal-maxilla at the level of the left orbit and nasal-premaxilla sutures) and some remaining partly open (e.g. maxilla-premaxilla and frontal-nasal sutures) suggests that IRSNB M.2343 corresponds to a young, physically immature individual.

Comparison and discussion

IRSNB M.2343 is herein not compared to *Belonodelphis peruanus* and *Incacetus broggii*, as the holotypes of these species lack preserved areas that overlap with the specimen described herein, and can thus not be compared with the latter.

IRSNB M.2343 can be identified as a delphinidan and can be excluded from the families Lipotidae, Iniidae, Pontoporiidae, Monodontidae and Odobenocetopsidae for the same anatomical features proposed for IRSNB M.2342. It differs from Albireonidae in lacking a steep posterior wall of the bony nares, formed by the flattened premaxillae, maxillae and frontals and from Phocoenidae in lacking a narrow posterior termination of the premaxilla and lacking a frontal boss on the skull vertex (Barnes 2008; Colpaert et al. 2015; Marx et al. 2016).

Among other Miocene early delphinidans, it differs from *Cammackacetus hazenorum, Hadrodelphis calvertense, Macrokentriodon morani* and *Miminiacetus pappus* in its markedly smaller skull size; from *C. hazenorum*, *H. calvertense, Lophocetus* spp., *Pithanodelphis cornutus* and *Tagicetus joneti* in its posteriorly less steeply ascending nasal portion of the premaxilla (ca. 30° to the horizontal plane in IRSNB M.2343); from *Atocetus* spp., *Ha. calvertense*, *Mi. pappus, Pictodelphis kidwellae*, *Pit. cornutus*, *Platysvercus ugonis* and *Sarmatodelphis moldavicus* in lacking any evidence for a conspicuous transverse constriction on the skull vertex; from *Mi. pappus, Sa. moldavicus, Sophianaecetus commenticius* and *Wimahl chinookensis* in its tabular skull vertex; from *Kampholophos serrulus, Lophocetus* spp., *Pic. kidwellae, Pit. cornutus, Pl. ugonis, So. commenticius* and *T. joneti* in its slightly anteromedially oriented, subrectangular nasal; from *Atocetus* spp. and *Wi. chinookensis* in its proportionally much smaller nasal; from *Rudicetus squalodontoides* in the anteroposterior length of its frontals not exceeding that of the nasal on the skull vertex; and from *Herbeinodelphis nancei* in the shorter anterior extent of the frontal anterior to the ventralmost point of the preorbital process, in lateral view.

IRSNB M.2343 shows some similarity to *Westmorelandelphis tacheroni* in its facial morphology, displaying for instance also a prominent, wide, and anterolaterally directed lacrimomaxillary fossa; a similarly gently arched orbit roof; and, as far as preserved, a slightly transversely concave premaxillary sac fossa, with a raised medial margin and a convex lateral margin. It differs however from this species in e.g. the anteroposteriorly shorter nasal, the absence of a vertical notch on the anterior face of the nasal, the lacrimal being more massive in lateral view, and in the posterolateral margin of its premaxilla being straight and anterolaterally oriented. The holotype specimen of *We. tacheroni* has a Serravallian age and is thus younger than IRSNB M.2343 (Godfrey & Lambert 2023).

Among the members of the species-rich genus *Kentriodon* it differs from *K. diusinus, K. hobetsu* and *K. 'obscurus'* in its more massive lacrimal, in lateral view; from *K. schneideri* in the posteriorly less steeply ascending nasal portion of the premaxilla; from *K. diusinus, K. hobetsu* in the anteroposteriorly shorter skull vertex; from *'K. hoepfneri'*, *K. nakajimai*, *K. pernix* and *K. sugawarai* in the medially and slightly anteriorly directed, subrectangular nasal; from '*K. hoepfneri'*, *K. nakajimai*, *K. pernix* in lacking a vertical notch on the anterior face of the nasal; and from *K. hobetsu, K. pernix, K. sugawarai* in the straight and anteromedially oriented nasal-frontal suture.

IRSNB M.2343 shows significant similarity to *Brevirostrodelphis dividum* in its dimensions and similar facial morphology. It shares for instance an overall highly similarly shaped orbit; a prominent, wide and anterolaterally directed lacrimomaxillary fossa; anteroposteriorly long bony nares; a straight and anterolaterally directed posterolateral margin of the premaxilla; a low, tabular and wide skull vertex; and a subrectangular, anteromedially directed nasal with an anterolateral process. It differs however from *B. dividum* in the more massive lateral exposure of its lacrimal; the more prominent wide and flat-topped

Dimension	*Brevirostrodelphis* sp. (IRSNB M.2343)	*Brevirostrodelphis dividum* (USNM 7278)
Anteroposterior length of lateral exposure of left lacrimal	18.5	14
Maximum dorsoventral thickness of left lacrimal + frontal + maxilla, in lateral view	23	14.5
Length of orbit (anteroposterior distance between ventral tip of postorbital process and ventral tip of preorbital process)	+50.5	48.5
Combined dorsoventral thickness of left frontal + maxilla, at mid-length of orbit	13.5	3
Dorsoventral thickness of left maxilla at postorbital process	3	2
Dorsoventral length of left preorbital process of frontal	11	9
Dorsoventral length of postorbital process	+18.5	*29
Transverse width of right nasal	26	20.5
Anteroposterior length of right nasal	20	18
Transverse width of right premaxilla, at anterior margin of nasal	27	26

Tab. 2 - Measurements (in mm) for *Brevirostrodelphis* sp. IRSNB M.2343 and *Brevirostrodelphis dividum* USNM 7278 (holotype). '+' indicates a minimal value. '*' indicates measurements taken from True (1912). Other measurements for *B. dividum* USNM 7278 are taken on a cast of this specimen housed at the IRSNB.

maxillary crest; the more massive maxilla and frontal in the orbit region (Tab. 2); the smaller anterolateral process of its nasal; and the less anteriorly oriented medial part of the anterior face of the nasal. The holotype specimen of *B. dividum* has presumably a Burdigalian age (see comparison section for IRSNB M.2342) and is thus older than IRSNB M.2343.

IRSNB M.2343 differs from *Brevirostrodelphis* aff. *B. dividum* IRSNB M.2342 in e.g. the rectangular shape of the right nasal and of the dorsomedial exposure of the frontal on the skull vertex and in possessing an anterolateral process of the right nasal.

Since both IRSNB M.2343 and USNM 7278 (holotype of *B. dividum*) presumably represent ontogenetically young specimens and have similar cranial dimensions, these differences are more difficult to explain through a significantly different ontogenetic stage. Taking account of individual variation in extant delphinidans (see e.g. Perrin 1975), other forms of intraspecific variation (including sexual dimorphism) may also fail to explain these differences. IRSNB M.2343 is therefore regarded here to potentially represent a new species of *Brevirostrodelphis*. Pending the discovery of new and more complete conspecific specimens from the North Sea Basin, preferentially including the ear bones, we provisionally identify this specimen as *Brevirostrodelphis* sp.

Family Kentriodontidae Slijper, 1936 (sensu Lambert et al. 2021)
Genus *Kentriodon* Kellogg, 1927

Kentriodon sp.

Figs. 8-11, Tab. 3

Referred specimen: IRSNB M.372, a partial cranium preserved in three major parts.

Locality: IRSNB M.372 was found during excavation works in the Antwerp area (northern Belgium), most probably during the building of fortifications around the city between 1860 – 1862 (Abel 1905; du Bus 1872). No precise locality is available, but the specific epithet '*scheynensis*' however refers to the Schijn river, which flows in an east-westwards direction into the Scheldt river in Antwerp. It can therefore be inferred that IRSNB M.372 was most likely collected from a location in the northeastern to eastern part of the Antwerp area, possibly in the Borgerhout or Deurne district (see map in Vanden Broek (1878)).

Horizon and age: The exact stratigraphic position of IRSNB M.372 is not known. It was however originally assigned to the 'crag d'Anvers' by du Bus (1872) and later to the Bolderian stage by Abel (1905) and to the Antwerpian stage ('Sables d'Anvers') by Misonne (1958) (see Laga & Louwye (2006) for an overview of these disused Neogene regional stages). It can subsequently be inferred that IRSNB M.372 possibly originates from the Antwerpen Member of the Berchem Formation and can therefore be tentatively assigned a Langhian to mid-Serravallian age (De Meuter & Laga 1976; Louwye et al. 2020), though an origin in any of the two other, geologically older, members of the Berchem Formation cannot be excluded.

Remarks: The cranium IRSNB M.372 was first formally, but briefly, described by du Bus (1872) who placed it in the new species *Phocaenopsis scheynensis*, without referring any other material to that species. Abel (1905) later assigned the specimen to the new combination *Acrodelphis scheynensis*, briefly redescribed the specimen, and listed a series of vertebrae together with the cranium as the type material. He also referred to this species 23 additional specimens from the Antwerp area, including vertebrae and limb bones, but no crania. In his work, Abel (1905) also provided two figures of the cranium (lateral and dorsal view) and noted the high similarity of the associated vertebrae with those of *Acrodelphis letochae* (Brandt, 1873) (based on undiagnostic material) from the Vienna basin. The vertebrae associated with the type cranium by Abel (1905) could not be found in the collection and are now considered lost. As they were never figured, the attribution of any other postcranial material to *A. scheynensis* cannot be tested anymore, not mentioning the relatively low diagnostic value of odontocete vertebrae. Kellogg (1927) noted the high similarity of the cranium of *A. scheynensis* with *Kentriodon pernix*, mainly at the level of the vertex. He also noted differences between the

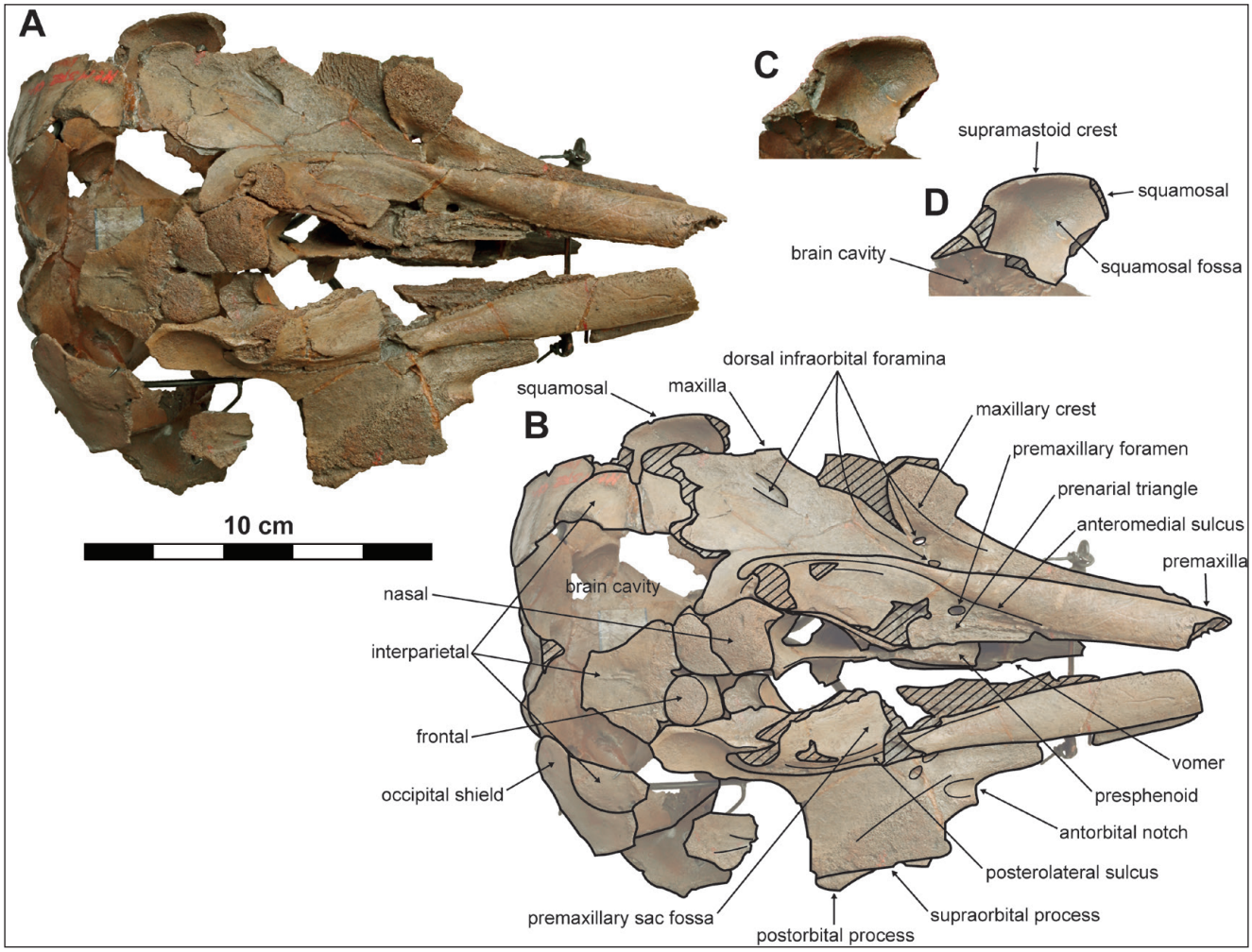

Fig. 8 - Dorsal views of the fragmentary cranium of *Kentriodon* sp. IRSNB M.372. A) Dorsal view cranium, photograph, and B) corresponding interpretative line drawing. C) Dorsal view left squamosal, photograph, and D) corresponding interpretative line drawing. Parallel lines indicate areas of breakage.

two species however, including the greater width of the premaxilla at the level of the antorbital notch in *A. scheynensis*. Fordyce & Muizon (2001) argued that the type cranium of *A. scheynensis* could better be placed close to, or within, *Kentriodon* due to the tabular shape of its skull vertex and the V-shaped anterior face of its nasal. Kazár & Hampe (2014) compared '*Kentriodon hoepfneri*' with IRSNB M.372 and noted the high similarity of the morphology of their nasals. They also noted that the posterior margin of the nasal of '*K. hoepfneri*' is more similar to IRSNB M.372 than to *K. pernix*. Kazár & Hampe (2014: fig. 9) also provided a comparative figure of the nasals of '*K. hoepfneri*', *K. pernix* and IRSNB M.372.

Description

General state of preservation. The cranium is fragmentarily preserved in three major parts. The first part consists of the left premaxilla, maxilla and frontal, the presphenoid and vomer, the skull vertex (right nasal and the dorsal exposure of both frontals), fragments of the interparietal and a fragment of the supraoccipital. The second part consists of the right premaxilla, maxilla and frontal. The third part consists of the basioccipital, both exoccipitals and both squamosals.

Premaxilla. The apical part of the rostrum is not preserved. The rostral parts of the left and right premaxilla are preserved for respectively 7.5 cm and 6.5 cm. The right premaxilla is for a large part broken medial to the anteromedial and posterolateral sulci. The dorsal surfaces of the nasal processes of both premaxillae, made of spongy bone, are abraded, but more so for the right than for the left premaxilla. The premaxillae as preserved are symmetrical. At the rostrum base, the dorsal surface of the premaxilla is transversely convex and faces dorsally. From the rostrum base towards the apex, the

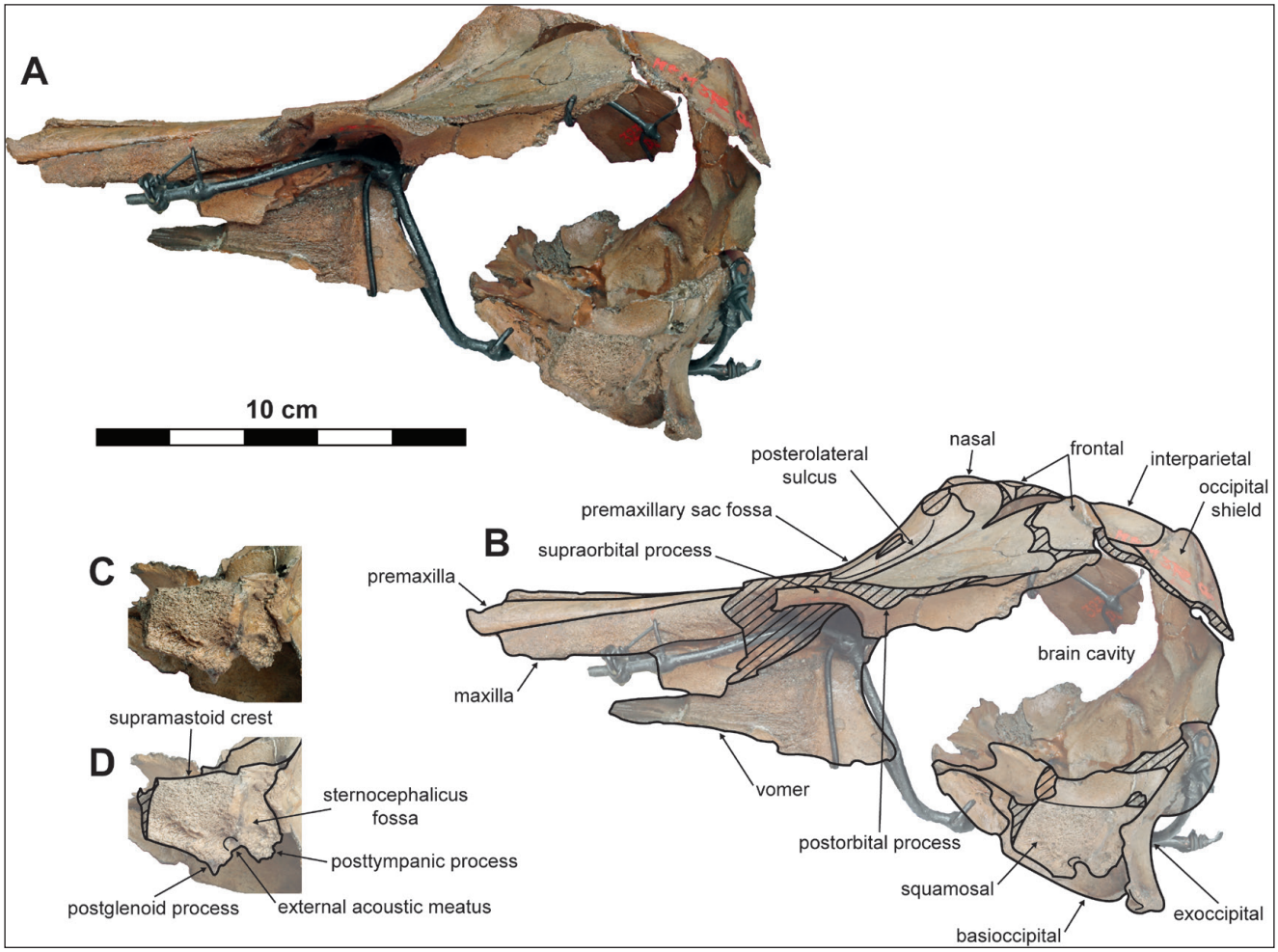

Fig. 9 - Left lateral view of the fragmentary cranium of *Kentriodon* sp. IRSNB M.372. A) Left lateral view cranium, photograph, and B) corresponding interpretative line drawing. C) Lateral view left squamosal, photograph, and D) corresponding interpretative line drawing. Parallel lines indicate areas of breakage.

dorsal surface of the premaxilla becomes gradually more laterally declined. The preserved left premaxillary foramen is located slightly posterior to the level of the antorbital notch and just medial to the mid-width of the premaxilla. This foramen opens dorsally and is elliptical in outline. The anteromedial sulcus is clearly delineated. The prenarial triangle forms a depression on the dorsal face of the premaxilla and has a rough, transversely concave dorsal surface. The posteromedial sulcus is shallow and poorly defined. The posterolateral sulcus is shallow but better defined, and extends posteriorly to the base of the nasal process of the premaxilla. The premaxillary sac fossa is transversely very slightly concave, appearing almost flat (Fig. 10). Lateral to the bony nares the premaxillary sac fossa is tabular and dorsally elevated above the maxilla, appearing as a moderately elevated plateau that extends to the posteriormost margin of the premaxilla. At the lateral margin of this plateau, the dorsal face of the premaxilla turns abruptly lateroventrally. The lateral margin of the premaxilla in the facial region is only very slightly laterally convex, appearing almost straight in dorsal view. At the level of the anterior dorsal infraorbital foramen, the lateral margin of the premaxilla is very slightly laterally concave over a distance of ca. 29 mm (Fig. 8). The nasal process terminates posteriorly against the anterolateral face of the nasal. The posterior margin of the nasal process is cut by the erected and anterolaterally directed medial edge of the maxilla. This medial edge of the maxilla is probably largely exposed due to the abrasion of this part of the dorsal face of the nasal process for both premaxillae.

Maxilla. Both maxillae are preserved in the basal part of the rostrum, to about the same level of their associated premaxillae. The lateral faces of the rostral parts of both maxillae are abraded to

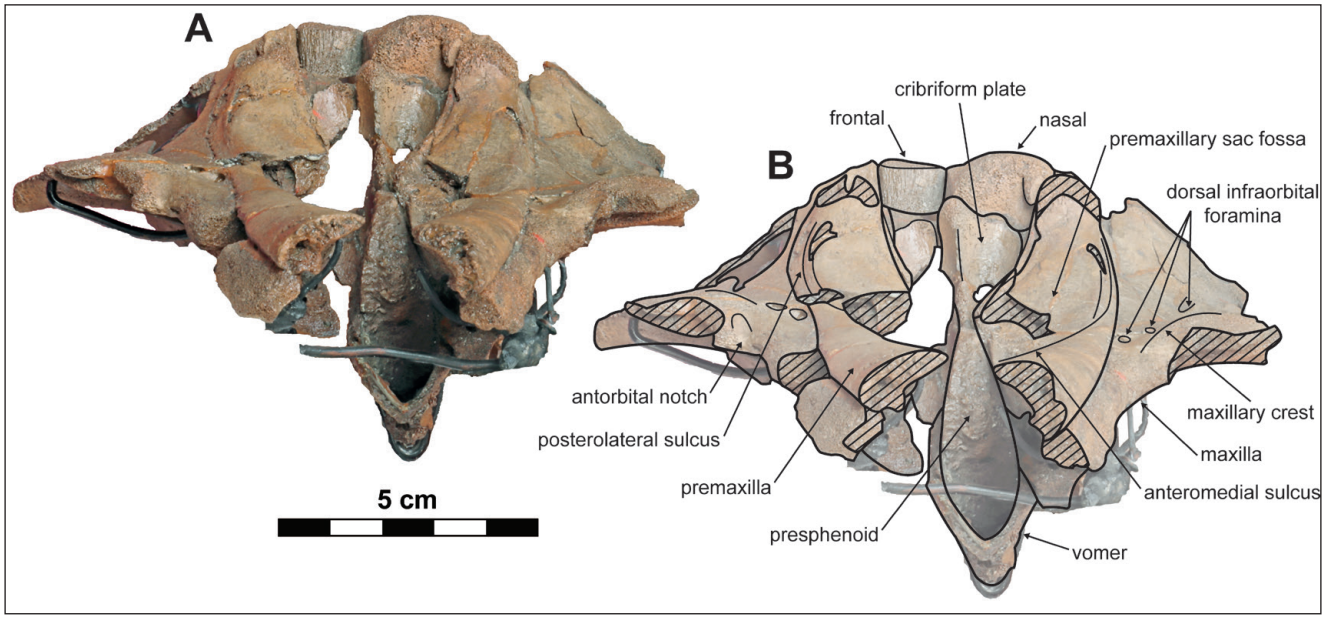

Fig. 10 - Anterior view of the fragmentary cranium of *Kentriodon* sp. IRSNB M.372. A) Anterior view, photograph, and B) corresponding interpretative line drawing. Parallel lines indicate areas of breakage. Note that the posterior fragment (basicranium) has been left out in this view.

some degree. Both antorbital processes are largely missing and only the medial margin of the right antorbital notch is preserved. The dorsal surfaces of both maxillae are slightly abraded in the supraorbital region. On the left side, the maxilla is missing for a large part in the orbital and antorbital area, due to breakage. The posterolateral part of the right maxilla is largely missing. At the rostral base, the dorsal surface of the maxilla is transversely flat and dorsally exposed lateral to the premaxilla for 10 mm. Due to the abrasion of the lateral face of the maxillae in the region anterior to the rostral base, the original lateral extent of the maxillae on the rostrum is unknown. Nonetheless, the lateral face of the maxilla steeply declines laterally in its rostral portion. Even though the antorbital notch is not completely preserved, the preserved medial and posterior walls suggest that it was originally anteriorly to anteroventrally directed. In the antorbital and supraorbital region, the dorsal surface of the maxilla is transversely and anteroposteriorly flat, except for a slight dorsal elevation corresponding to a low, anteromedially directed maxillary crest. This maxillary crest is present on both maxillae and extends from the postorbital region to the base of the antorbital notch. Medially, the maxilla is narrowly dorsally exposed along the lateral margin of the bony nares (Fig. 8). This medially located dorsal exposure of the maxilla very gradually widens towards the anterior part of the bony nares. Two closely spaced anterior dorsal infraorbital foramina are present on both maxillae. The first, anteriormost of these dorsal infraorbital foramina is situated just posterior to the level of the left premaxillary foramen and just lateral to the maxilla-premaxilla suture. The second of these dorsal infraorbital foramina is situated just posterolateral to the first one. Both anterior dorsal infraorbital foramina are similar in size (4-5 mm in anteroposterior diameter) and open laterally. A posterior dorsal infraorbital foramen is present on both maxillae at the level of the posterior margin of the bony nares and 16 mm lateral to the maxilla-premaxilla suture. Posteromedially, the maxilla terminates against the posterolateral margin of the nasal and the lateral margin of the dorsomedial exposure of the frontal along the skull vertex. At the contact with the posterolateral margin of the nasal, the maxilla abruptly rises dorsally but does not dorsally reach the same elevation as the dorsal surface of the nasal.

Presphenoid. The presphenoid fills the proximal part of the mesorostral groove for ca. 5.5 mm anterior to the right premaxillary foramen, reaching just anterior to level of the antorbital notch. In dorsal view the nasal septum is thin and rectilinear. Since a part of the nasal septum is broken it is unclear to which extent it originally extended anterodorsally.

It appears however that it probably did not extend much dorsally above the maxillae and premaxillae.

Vomer. The apical part of the vomer is broken. At the base of the rostrum, the vomer makes the thin ventral and lateral walls of the mesorostral groove; at this level the groove has a dorsoventrally elongated drop shaped cross section with a pointed base (Fig. 10).

Nasal. Only the left nasal is preserved on the skull vertex. In dorsal view it has an overall pentagonal outline and is approximately as wide transversely as it is long anteroposteriorly. The dorsal surface of the nasal is slightly domed and slopes anteromedially towards the internasal suture, indicating the presence of a well-developed internasal fossa (Fig. 10). The internasal suture is straight and oriented anteroposteriorly. A deep, sharp, vertical notch is present in the lateral part of the anterior face of the nasal. This notch opens anteromedially and defines a pointed, narrow and anteriorly oriented anterolateral process of the nasal. More medially, the anterior margin of the nasal is directed slightly anteromedially in dorsal view. The posterolateral margin of the of the nasal is posteriorly drawn into a short, sharp protrusion in dorsal view. The nasal-frontal suture is directed anteromedially and shows only a slight posteriorly convex undulation.

Frontal. The pre- and postorbital processes of both frontals are missing for the most part. The lateral margin of the supraorbital process is only preserved on the right frontal. Due to abrasion in this region, it is unclear how much of the frontal was originally dorsally exposed in the orbital region. Based on the impression of the partly abraded maxilla on the right supraorbital process however, it can be inferred that most of the region of the supraorbital process was dorsally covered by the maxilla. The lateral margin of the right supraorbital process is concave in dorsal view and is oriented very slightly anteromedially. The base of the right postorbital process is slender, less than 7 mm in anteroposterior length. The preorbital process was originally thin, estimated to have been less than 8 mm in dorsoventral thickness. Posterior to the left maxilla, the frontal was originally dorsally exposed for about 11 mm before the barely marked nuchal crest (Figs. 8 & 9). Part of the dorsal exposure of the frontal as preserved is due to the incomplete preservation of the posterior edge of the maxilla in this region. The slightly dorsally convex dorsal exposure of the frontals on the skull vertex are asymmetrical, with the left frontal being transversely wider and extending further anteromedially than the right frontal. The posterolateral angle of this left dorsomedial exposure of the frontal is broken. The anterior face of the unexpectedly shorter right frontal on the skull vertex shows no signs of damage, possibly indicating that its anterior face was bounded by the missing right nasal, or by a not completely fused anteromedial part of the frontal itself. In the former case this would indicate that the nasals are also asymmetric in their dorsal outline. The anterior face of right frontal on the skull vertex is anteriorly convex and its overall dorsal outline is elliptical. The outline of the left frontal on the skull vertex is subtriangular. The anteromedial angle of the left frontal on the skull vertex is pointed and originally extended anteromedially between the nasals. The interfrontal suture is rectilinear and oriented anteroposteriorly. The dorsal surface of each frontal is slightly dome shaped and slopes anteromedially, but less than the dorsal surface of the nasal. Together with the nasals, the frontals make a pentagon-shaped and tabular skull vertex.

Interparietal. The interparietal is a relatively large bone in delphinidans, situated anterior to the supraoccipital, medial to the parietals and posterior to the frontals, which generally fuses early during ontogeny with the supraoccipital (see Mead & Fordyce (2009) and Roston & Roth (2019)). The interparietal is preserved in three fragments: a left, medial and right fragment (Fig. 8). The dorsomedial region of the interparietal, just posterior to the frontals on the skull vertex, is horizontal, with a slight medial depression pierced by tiny foramina. The frontal-interparietal suture on the vertex is oriented slightly anteromedially. Best seen on the right-side fragment, the interparietal-supraoccipital suture is posteriorly convex, with the interparietal being distinctly dorsally thicker than the supraoccipital. There is no marked nuchal crest detected along the preserved regions.

Supraoccipital. The supraoccipital is only fragmentarily preserved. Anterolaterally, the occipital shield is strongly anteroposteriorly convex.

Squamosal. Both squamosals are partly preserved with most of the falciform processes and the anterior part of the zygomatic processes missing (more so on the right side). The supramastoid crest is sharp and prominent, oriented anteroposteriorly, and has a slightly laterally convex lateral margin.

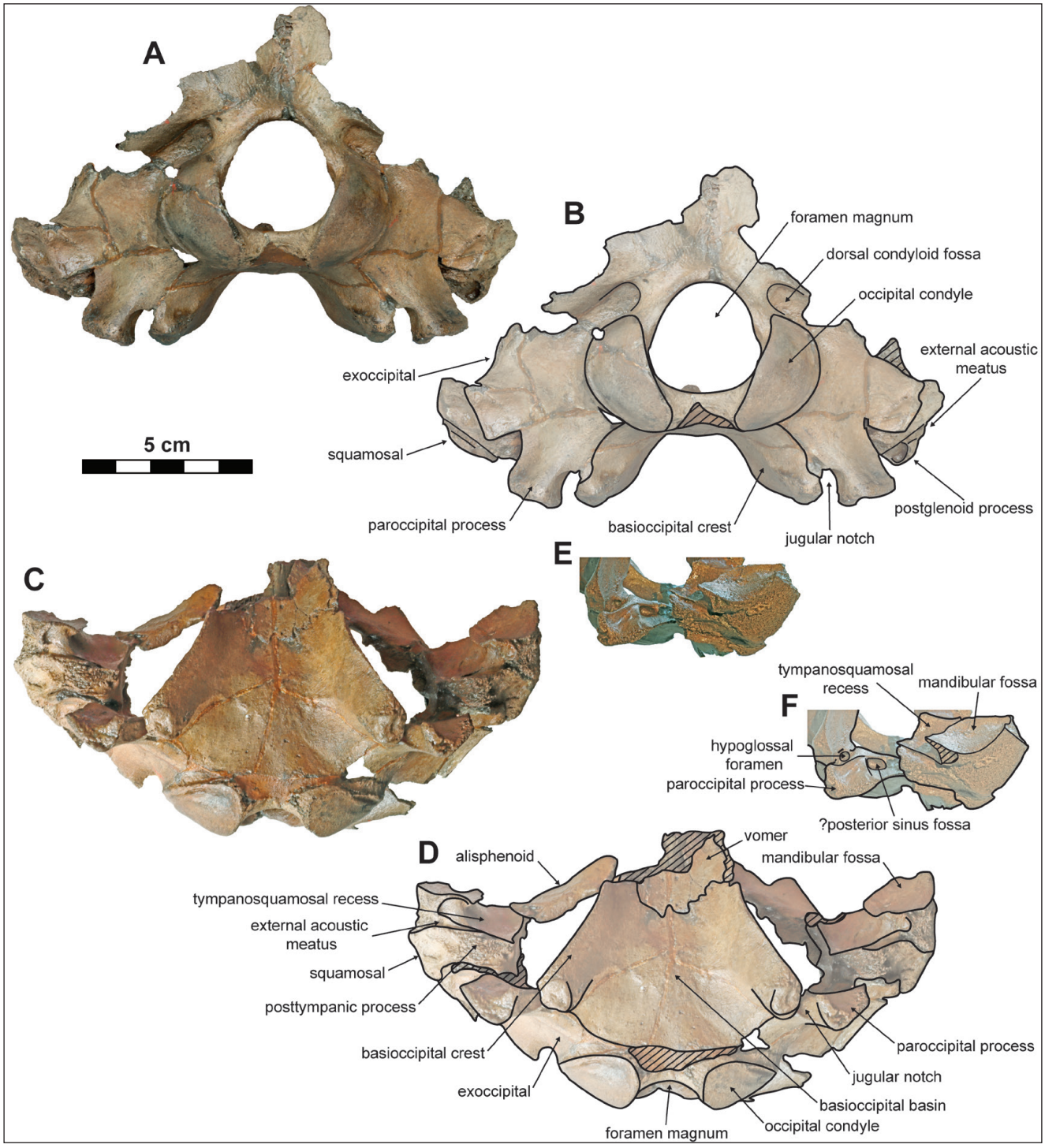

Fig. 11 - Posterior and ventral views of the basicranium (posterior fragment) of *Kentriodon* sp. IRSNB M.372. A) Posterior view, photograph, and B) corresponding interpretative line drawing. C) Ventral view, photograph, and D) corresponding interpretative line drawing. E) Anteroventrolateral view of the left side of the basicranium, photograph, and F) corresponding interpretative line drawing. Parallel lines indicate areas of breakage.

The squamosal fossa forms a reniform, deep and smooth depression (Fig. 8). Towards its posterior margin, the surface of the squamosal fossa rises dorsally more gently than towards the supramastoid crest. The mandibular fossa as preserved (Fig. 11C - F) is moderately concave anteroposteriorly; in its ventral part it is slightly transversely concave, becoming more concave anterodorsally. The posterior part of the mandibular fossa faces anteroventrally, while it faces more medially in its anterior portion.

The medial margin of the mandibular fossa is thin and sharp, underhanging the tympanosquamosal recess. The lateral part of the postglenoid process is broken on the left side, but the right process is complete. In lateral view the postglenoid process is ventrally directed, V-shaped, with a sharp ventral edge. Ventrally, it does not reach the level of the ventral margin of the basioccipital crest, being even shorter than the paroccipital process. The broad and deep medial part of the tympanosquamosal recess is flat and faces more ventrally than the mandibular fossa. In its posteroventral region, it extends laterally along the medial surface of the postglenoid process, where it forms a deep, dorsolaterally elongated notch (Fig. 11C & D), further deepening on the posterior face of the process, just anterior to the external acoustic meatus. This extension of the recess gives the impression of a broad, subrectangular lateral outline of the meatus, but the latter is actually a narrow (1 mm) groove defined anteriorly by a thin and low crest. The short posttympanic process is made of laminar bone, directed posteroventrally, and does not extend below the postglenoid process. The posterolateroventrally facing sternocephalicus fossa (Fig. 9C & D) is shallow, partly subdivided by a low subhorizontal ridge, and does not extend anterior to the level of the external acoustic meatus.

Exoccipital. Both exoccipitals are largely preserved. The paroccipital process extends ventrally slightly below the basioccipital crest (Fig. 11A & B). The lateralmost region of the posterior surface of the exoccipital, along the suture with the squamosal, is marked by an acute oblique crest, directed dorsolaterally and slightly longer on the right side, which probably corresponds to the attachment area for neck muscles. The occipital condyles are relatively wide and are directed dorsolaterally, with a nearly indistinct condylar neck. The dorsal condyloid fossae are deep. The foramen magnum is subtriangular in outline and is as high as wide. A deep, pocket-like elliptical fossa (Fig. 11E & F), presumably for the posterior sinus, is present on the anterior face of the exoccipital, just dorsomedially to the posterolateral sinus crest of the paroccipital process. The deep (8 mm) jugular notch terminates dorsomedially into the circular hypoglossal foramen.

Basioccipital. The basioccipital is completely preserved. Medially the basioccipital basin is slightly domed. The lateral faces of the basioccipital crests are anteroposteriorly and dorsomedially slightly laterally concave in lateral view. Posteroventrally the basioccipital crest gradually increases in width and terminates in a posteroventrally facing rough, flat surface (Fig. 11C & D). This rough surface is followed anterodorsomedially on the medial surface of the basioccipital crest by a sharp crest that lowers after turning more medially towards the sagittal plane of the basioccipital basin.

Ontogeny and size estimation

The subtriangular shape of the foramen magnum and the open (e.g. premaxilla-nasal) as well as not completely fused (e.g. interparietal-frontal, nasal-frontal and maxilla-premaxilla) cranial sutures indicate that IRSNB M.372 represents a young, possibly newborn individual. Indeed, in the extant delphinid *Stenella attenuata* the foramen magnum is also subtriangular in newborn specimens, becoming, to varying degree, more oval with development (Perrin 1975). The subtriangular shape of the foramen magnum of IRSNB M.372 thus also possibly points to a young ontogenetic age of this specimen. Based on its bizygomatic width (Tab. 3), the total body length of IRSNB M.372 is estimated to 1.24 m, using the equation provided by Pyenson & Sponberg (2011) for stem delphinoids. It should be noted however that the equations provided by the latter authors were determined for adult specimens. As allometric growth most likely impacts cranial proportions, this size estimation remains approximate.

Comparison and discussion

IRSNB M.372 is herein not compared to *Belonodelphis peruanus*, *Herbeinodelphis nancei* and *Incacetus broggii*, as the holotypes of these species lack preserved areas that overlap with the specimen described herein, and can thus not be compared with the latter.

IRSNB M.372 can be identified as a delphinidan and can be excluded from the families Lipotidae, Iniidae, Pontoporiidae, Albireondidae, Phocoenidae, Delphinidae and Odobenocetopsidae for the same anatomical features proposed for IRSNB M.2342. It differs from Monodontidae in the drastically smaller dorsomedial exposure of its maxillae along the bony nares.

Among other Miocene early delphinidans, it differs from *Cammackacetus hazenorum*, *Hadrodelphis calvertense*, *Macrokentriodon morani* and *Miminiacetus*

pappus in its drastically smaller skull size; from *Brevirostrodelphis dividum*, *Kampholophos serrulus, Lophocetus* spp., *Ma. morani* and *Mi. pappus* in the almost straight lateral margin of its premaxilla in the facial region; from *C. hazenorum*, *H. calvertense*, *Pithanodelphis cornutus* and *Tagicetus joneti* in the posteriorly less steeply ascending nasal portion of the premaxilla (slope of dorsal surface of nasal portion of premaxilla relative to horizontal plane in lateral view equals ca. 45° in IRSNB M.273); from *Westmorelandelphis tacheroni* and *Wimahl chinookensis* in its pentagonal skull vertex; from *Atocetus* spp., *H. calvertense*, *Mi. pappus, Pictodelphis kidwellae, Pit. cornutus*, *Platysvercus ugonis* and *Sarmatodelphis moldavicus* in lacking a marked transverse constriction on the skull vertex; from *B. dividum*, *C. hazenorum*, *K. serrulus*, *Lophocetus* spp., *Pic. kidwellae*, *Pit. cornutus*, *Pl. ugonis*, *Rudicetus squalodontoides*, *Sophianaecetus commenticius, We. tacheroni* in its equidimensional, pentagonal left nasal; from *R. squalodontoides* and *Wi. chinookensis* in possessing a vertical notch on the anterior face of its nasal; and from *Atocetus* spp. and *Wi. chinookensis* in its proportionally much smaller nasal.

It differs from *Brevirostrodelphis* aff. *B. dividum* IRSNB M.2342 and *Brevirostrodelphis* sp. IRSNB M.2343 in e.g. its pentagonal left nasal, possessing a vertical notch on the anterior face of its nasal, the tabular morphology of its premaxillary sac fossa and the straight lateral margin of the nasal portion of its premaxilla.

Among the members of the species rich genus *Kentriodon* it differs from *K. hobetsu* and *K. sugawarai* in the straight lateral margin of its premaxillary sac fossa; from *K. diusinus* and *K. hobetsu* in the anteroposteriorly relatively shorter skull vertex; from *K. schneideri* in the posteriorly less steeply ascending nasal portion of the premaxilla; from *K. diusinus* in the left nasal that is posterolaterally bounded by the maxilla; and from *K. sugawarai* in the pentagonal outline of the left nasal.

As mentioned above, the similarity in the morphology of the nasals of IRSNB M.372 and '*K. hoepfneri'* is already discussed by Kazár & Hampe (2014) (see also comments on this species by Nobile et al. (2024)). They also note some differences between '*K. hoepfneri'* and IRSNB M.372 however, including the anteromedially globose nasal and the larger combined thickness of the supraorbital process of the frontal and its associated maxilla of '*K. hoepfneri*'. These differences are corroborated herein. The holotype of '*K. hoepfneri'* has a latest Middle to early Late Miocene age and is thus presumably younger than IRSNB M.372 (Kazár & Hampe 2014).

IRSNB M.372 also shows some resemblance to *K. nakajimai* at the level of the skull vertex, i.e. the rather similar dorsal outline of its left nasal (best compared to the paratype specimen) and the triangular dorsal exposure of its left frontal. It differs however from this species in e.g. its longer internasal suture; the sharper anterolateral process of its nasal; its proportionally anteroposteriorly longer skull vertex; and its maxillary crest that anteriorly reaches medial to the antorbital notch and is symmetrical on both sides of the skull. The holotype of *K. nakajimai* has a latest Middle to earliest Late Miocene age and is thus presumably younger than IRSNB M.372 (Kimura & Hasegawa 2019).

IRSNB M.372 shows much similarity to *K. 'obscurus'* in its size and cranial morphology, differing only in details (see also comments on *K. 'obscurus'* LACM 21256 by Nobile et al. (2024)). Differences between both specimens however include e.g. the larger premaxillary width of IRSNB M.372 anterior to middle of the supraorbital process (Tab. 3); the larger width of its bony nares (Tab. 3); its maxilla that completely covers the supraorbital process of the frontal in dorsal view; and the smaller combined thickness of its maxilla and frontal in the orbital region (Tab. 3). Like IRSNB M.372, *K. 'obscurus'* specimen LACM 21256 displays open sutures, indicating that it also represents a juvenile specimen. These differences are therefore difficult to explain by a differing developmental stage. *K. 'obscurus'* specimen LACM 21256 has approximately an early Middle Miocene age and thus possibly overlaps in stratigraphic age with IRSNB M.372 (Barnes & Mitchell 1984).

As mentioned earlier, the close resemblance of IRSNB M.372 to *K. pernix* (type species of *Kentriodon*) has already been noted by previous authors (Kellogg 1927; Fordyce & Muizon, 2001). The high similarity of IRSNB M.372 to *K. pernix* is here confirmed not only at the level of its skull vertex, but also in its overall cranial morphology and skull size. Differences between IRSNB M.372 and *K. pernix* are however present, including e.g. the larger width of its premaxilla at the level of the antorbital notch (as already observed by Kellogg (1927)) and posteriorly to a level at ca. the postorbital process (Tab.

Dimension	*Kentriodon* sp. (IRSNB M.372)	*Kentriodon* '*obscurus*' (LACM 21256)	*Kentriodon pernix* (USNM 10670)
Width of rostrum at antorbital notch	e68	**67.7	*65
Transverse width of left premaxilla at antorbital notch	19.5	e14.5	18
Transverse width of right maxilla at antorbital notch	11.5	e14	13
Transverse width of right maxilla at preorbital process	e29	e32.5	36
Transverse width of left premaxilla at preorbital process	e23.5	e17.5	17
Maximal dorsoventral thickness of right lacrimal + frontal + maxilla, at preorbital process	+8.5	e17	17
Transverse distance between lateral margins of premaxillae at preorbital process	e55.5	e38.5	38
Transverse width of left premaxilla at middle of supraorbital process	e21.5	e22	17.5
Transverse width of right maxilla at middle of supraorbital process	e29.5	e30	+22
Maximal dorsoventral thickness of right frontal + maxilla at middle of supraorbital process	6	e11	16
Transverse width of right maxilla at postorbital process	e34	e31	e41.5
Transverse width of left premaxilla at postorbital process	19	e16	17
Dorsoventral length of postorbital process	+6	e13.5	e17
Transverse distance between lateral margins of premaxillae at postorbital process	e59.5	e48.5	52.5
Largest transverse width of premaxilla	e23	e24	25
Largest transverse width of bony nares	28	e19	e22
Transverse width of left nasal	20	-	17
Anteroposterior length of left nasal	17.5	-	20.5
Length of internasal suture	10	-	10.5
Anteroposterior length of left frontal on skull vertex	14	-	13
Transverse width of left frontal on skull vertex	e16	-	11.5
Anteroposterior length of right frontal on skull vertex	11	-	*12.2
Transverse width of right frontal on skull vertex	13	-	11.5
Anteroposterior length of skull vertex along sagittal plane	28	-	24
Largest bizygomatic width	+145	-	*,e142
Width of foramen magnum	29.5	-	*26.5
Height of foramen magnum	29	-	*21.5
Dorsoventral length of right occipital condyle	30	-	*31
Maximal transverse width of right occipital condyle	25	-	*21
Transverse width across occipital condyles	61.5	-	*54
Largest distance between lateral margins of basioccipital crests	67.5	-	59

Tab. 3 - Measurements (in mm) for *Kentriodon* sp. IRSNB M.372, *Kentriodon 'obscurus'* LACM 21256 and *Kentriodon pernix* USNM 10670 (paratype). '+' indicates a minimal value, 'e' indicates an estimate value and '-' indicates non-available data. '*' and '**' indicate measurements taken from Kellogg (1927) and Barnes & Mitchell (1984) respectively. Other measurements for *K. pernix* USNM 10670 were taken on a cast of this specimen housed at the IRSNB. Other measurements for *K. 'obscurus'* LACM 21256 were taken from true scale images of this specimen provided in Barnes & Mitchell (1984), which should consequently be interpreted cautiously.

3); the more angular lateral margin of its premaxillary sac fossa; the undulatory as opposed to angular shape of its nasal-frontal suture; and the more limited ventral extend of its paroccipital processes. As the holotype of *K. pernix* represents an immature individual, these differences are difficult to explain by a (large) difference in ontogenetic stage (Kellogg 1927). The holotype of *K. pernix* has a latest Early Miocene age and thus potentially overlaps in age with IRSNB M.273 (Kellogg 1927; Kidwell et al. 2015).

IRSNB M.372 differs from *Kentriodon* sp. MCAF-MB2, recently described from the early Burdigalian of northeastern Italy (Nobile et al. 2024), in its maxillary dimensions at the level of the rostrum, its markedly less distinct anteromedial, posteromedial and posterolateral sulci and the smaller dorsomedial exposure of its maxilla along the lateral margins of and anterior to the bony nares. *Kentriodon* sp. MCAF-MB2 has an early Burdigalian age and is thus presumably older than IRSNB M.372.

Differences between IRSNB M.372 and the recently described, cranially malformed specimen *Kentriodon* cf. *Kentriodon pernix* IRSNB M.2340 are mentioned in Lambert et al. (2025). The latter originates from the Antwerpen Member (Berchem Formation) in Antwerp (northern Belgium) and thus overlaps with IRSNB M.372 in geographic region and possibly also in age.

Due to its high similarity to *K. pernix* (type species) and to *K.* '*obscurus*' specimen LACM 21256, IRSNB M.372 is here assigned to *Kentriodon*. This attribution confirms the similarities of IRSNB M.372 with *K. pernix* as noted by Kellogg (1927), with '*K. hoepfneri*' as noted by Kazár & Hampe (2014) (but see comments on the affinities of the latter in Nobile et al. (2024)), and confirms the hypothesis of Fordyce & Muizon (2001) that IRSNB M.372 is close to or in the genus *Kentriodon*. Since IRSNB M.372 represents a juvenile and fragmentary specimen, we here restrain from defining a new species based on this specimen and simply identify it as *Kentriodon* sp., pending the discovery of more complete, preferentially physically mature conspecific specimens with preserved ear bones.

Palaeobiogeographic and palaeoecological discussion

In the North Atlantic realm, *Brevirostrodelphis* is currently only described from the late Early to early

Middle Miocene of the U.S. Atlantic Coastal Plain (Barwick 1939; Godfrey & Lambert 2023; Kidwell et al. 2015; True 1912). From the North Sea Basin, only very fragmentary records (two teeth) have tentatively been assigned to *Brevirostrodelphis* (Louwye et al. 2010; Everaert et al. 2019). The identifications of *Brevirostrodelphis* aff. *B. dividum* IRSNB M.2342 and *Brevirostrodelphis* sp. IRSNB M.2343 described herein, provide the first unambiguous records of *Brevirostrodelphis* from the North Sea Basin and demonstrate the transatlantic distribution of this genus during the Miocene. The redescription and reattribution of specimen IRSNB M.372 to *Kentriodon* sp., provides the fourth (including '*Kentriodon hoepfneri*') description of *Kentriodon* from the eastern side of the North Atlantic and the third from the North Sea Basin, based on cranial material (Kazár & Hampe 2014; Nobile et al. 2024; Lambert et al. 2025).

The description of the two *Brevirostrodelphis* specimens and one *Kentriodon* specimen herein, combined with their more fragmentary records (see Louwye et al. (2010) and Everaert et al. (2019)) and the recent description of *Kentriodon* sp. IRSNB M.2340 (see Lambert et al. (2025)), raises the question whether these were rather prevalent delphinidan genera in the southern North Sea Basin during the Miocene. This hypothesis, and the relative abundance of Miocene early delphinidans in the southern North Sea Basin in general, could be tested by studying the relative abundances of the often better preserved and more commonly found periotics from the IRSNB collection.

Another interesting observation is that two of the three specimens described herein represent juveniles. Interesting to note in this context is that another small early delphinidan from the Miocene of the North Sea Basin, *Pithanodelphis cornutus*, is represented by a single specimen (IRSNB M.373) that displays clues for a young ontogenetic stage: open nasal-maxilla suture, open internasal suture and loss of the right premaxilla, indicating that it was not yet fused to the maxilla (see Muizon (1988b: fig. 101)). Furthermore, the recently described, cranially malformed *Kentriodon* sp. IRSNB M.2340 displays similar features indicating a young ontogenetic stage (Lambert et al. 2025). Together, these observations raise the question whether the southern North Sea Basin might have served as a nursing ground or may have been favoured by relatively young individuals for several early delphinidan taxa during the Miocene and not simply reflects a possible higher mortality rate of juveniles. Such a pattern of habitat segregation in relation to ontogenetic stages and, in some cases, more specifically calving and nursing activities, has been reported for several extant odontocete species, including delphinidans (e.g. Martin & da Silva 2004; Hartman et al. 2014; Fontanesi et al. 2024). This hypothesis could be further explored by comparing the early delphinidan ratio of juveniles to adult specimens with that of eurhinodelphinids, which have a richer fossil record (e.g. Lambert 2005) and were presumably more coastal, residing more permanently in the southern North Sea Basin during the late Early to Middle Miocene. The same hypothesis could also be tested for the odontocetes from the Miocene deposits on the U.S. Atlantic Coastal Plain.

Conclusions

Fragmentary early delphinidan crania IRSNB M.2342 and IRSNB M.2343, found in lower Langhian deposits of the Antwerpen Member (Berchem Formation) in Berchem (Antwerp) are here described and provisionally identified as *Brevirostrodelphis* aff. *B. dividum* and *Brevirostrodelphis* sp. The description and identification of these specimens provide the first unambiguous records of this genus from the North Sea Basin and demonstrate its transatlantic distribution during the Miocene. The historical specimen IRSNB M.372 (type of *Phocaenopsis scheynensis*), collected in the Antwerp area most likely from Lower to Middle Miocene strata, is here redescribed and recombined as *Kentriodon* sp.

Based on the ratio of juvenile to adult specimens, the southern North Sea Basin is here provisionally hypothesized to have served as a favoured ground for young individuals of several early delphinidan species during the Miocene.

Data Availability Statement. The data supporting the results of this research are available upon request. Interested researchers may contact the corresponding author to obtain access.

Acknowledgements: We wish to thank Dave J. Bohaska, James G. Mead, John J. Ososky, and Charles W. Potter (USNM), Stephen J. Godfrey and John R. Nance (CMM), Larry G. Barnes and Vanessa R. Rhue (LACM), Sébastien Bruaux, Cécilia Cousin, Annelise Folie, and Olivier Pauwels (IRSNB) for providing access to the collections under their care. We would also like to thank the two reviewers, Toshiyuki Kimura and Margot Nelson, for their constructive comments and suggestions, which greatly helped improving a previous version

of this work. The bulk of the work on the studied fossil material has been undertaken during a Master thesis of PVR (at that time a Ghent University student) at the IRSNB, under the supervision of SL and OL.

References

Abel O. (1905) - Les Odontocètes du Boldérien (Miocène supérieur) d'Anvers. *Mémoires du Musée Royal d'Histoire Naturelle de Belgique*, 3: 1-155.

Barnes L.G. (1978) - A review of *Lophocetus* and *Liolithax* and their relationships to the delphinoid family Kentriodontidae (Cetacea: Odontoceti). *Bulletin of the Natural History Museum of Los Angeles County*, 28: 1-35.

Barnes L.G. (1985) - The Late Miocene dolphin *Pithanodelphis* Abel, 1905 (Cetacea: Kentriodontidae) from California. *Contributions in Science*, *Natural History Museum of Los Angeles County*, 367: 1-27.

Barnes L.G. (2008) - Miocene and Pliocene Albireonidae (Cetacea, Odontoceti), rare and unusual fossil dolphins from the eastern North Pacific Ocean. *Science Series*, *Natural History Museum of Los Angeles County,* 41: 99-152.

Barnes L.G. & Mitchell E.D. (1984) - *Kentriodon obscurus* (Kellogg, 1931), a fossil dolphin (Mammalia: Kentriodontidae) from the Miocene Sharktooth Hill Bonebed in California. *Contributions in Science, Natural History Museum of Los Angeles County*, 353: 1-23.

Barwick A.R. (1939) - Miocene Porpoise (Delphinodon dividum) from Southern Maryland. *The American Midland Naturalist*, 22: 154-159.

Bianucci G., Geisler J.H., Citron S. & Collareta A. (2022) - The origins of the killer whale ecomorph. *Current Biology*, 32: 1843-1851.

Boessenecker R.W. & Geisler J.H. (2023) - New Skeletons of the Ancient Dolphin *Xenorophus sloanii* and *Xenorophus simplicidens* sp. nov. (Mammalia, Cetacea) from the Oligocene of South Carolina and the Ontogeny, Functional Anatomy, Asymmetry, Pathology, and Evolution of the Earliest Odontoceti. *Diversity*, 15: 1154.

Calzada N., Aguilar A., Grau E. & Lockyer C. (1997) - Patterns of growth and physical maturity in the western Mediterranean striped dolphin, *Stenella coeruleoalba* (Cetacea: Odontoceti). *Canadian Journal of Zoology*, 75: 632-637.

Chen I., Chou L.S., Chen Y.J. & Watson A. (2011) - The Maturation of Skulls in Postnatal Risso's Dolphins (*Grampus Griseus*) from Taiwanese Waters. *Taiwania*, 56: 177-185.

Colpaert W., Bosselaers M. & Lambert O. (2015) - Out of the Pacific: A second fossil porpoise from the Pliocene of the North Sea Basin. *Acta Palaeontologica Polonica*, 60: 1-10.

Dawson S.D. (1996) - A New Kentriodontid Dolphin (Cetacea; Delphinoidea) from the Middle Miocene Choptank Formation, Maryland. *Journal of Vertebrate Paleontology*, 16: 135-140.

Deckers J. & Everaert S. (2022) - Distinguishing the Miocene Kiel and Antwerpen Members (Berchem Formation) and their characteristic horizons using cone penetration tests in Antwerp (northern Belgium). *Geological Journal*, 57: 2129-2143.

del Castillo D.L., Flores D.A. & Cappozzo H.L. (2014) - Ontogenetic Development and Sexual Dimorphism of Franciscana Dolphin Skull: a 3d Geometric Morphometric Approach. *Journal of morphology*, 275: 1366-1375.

De Meuter F.J. & Laga P.G. (1976) - Lithostratigraphy and biostratigraphy based on benthonic foraminifera of the Neogene deposits of Northern Belgium. *Bulletin Belgische Vereniging voor Geologie/Bulletin de la Société belge de Géologie*, 85: 133-152.

de Verteuil L. & Norris G. (1996) - Miocene dinoflagellate stratigraphy and systematics of Maryland and Virginia. *Micropaleontology*, 42, suppl., 1-172.

du Bus, B.A.L. (1872) - Mammifères nouveaux du Crag d'Anvers. *Bulletin de l'Académie Royale des Sciences, des Lettres et des Beaux-Arts de Belgique*, 34: 491-509.

Dybkjær K. & Piasecki S. (2010) - Neogene dinocyst zonation for the eastern North Sea Basin, Denmark. *Review of Palaeobotany and Palynology*, 161: 1-29.

Everaert S., De Schutter P., Mariën G., Cleemput G., Van Boeckel J., Rondelez D. & Bor T. (2019) - Een vroeg-Miocene fauna uit het Zand van Kiel (Formatie van Berchem) bij Post X in Berchem (Antwerpen). *Afzettingen, Werkgroep Tertiaire en Kwartaire Geologie*, 40: 83-100.

Everaert S., Munsterman D.K., De Schutter P.J., Bosselaers M., Van Boeckel J., Cleemput G. & Bor, T.J. (2020) - Stratigraphy and palaeontology of the lower Miocene Kiel Sand Member (Berchem Formation) in temporary exposures in Antwerp (northern Belgium). *Geologica Belgica*, 23: 167-198.

Everaert S., Deckers J., Bosselaers M., Schiltz M. & Louwye S. (2024) - A Neogene succession in the city centre of Antwerp (Belgium): stratigraphy, palaeontology and geotechnics of the Rubenshuis temporary outcrop. *Geologica Belgica*, 27: 47-70.

Fontanesi E., Ascheri D., Bertulli C.G., Salvioli F. & McGinty N. (2024) - Bottlenose dolphin (*Tursiops truncatus*) habitat partitioning in relation to age classes in the northwest Mediterranean Sea. *Marine Biology*, 171: 137.

Fordyce R.E. & Muizon C. de. (2001) - Evolutionary history of cetaceans: a review. In: Mazin J.-M. & de Buffrénil V. (Eds) - Secondary Adaptation of Tetrapods to Life in Water: 169-233. Verlag Dr. Friedrich Pfeil, München.

Galatius A. & Kinze C.C. (2003) - Ankylosis patterns in the postcranial skeleton and hyoid bones of the harbour porpoise (*Phocoena phocoena*) in the Baltic and North Sea. *Canadian Journal of Zoology*, 81: 1851-1861.

Gibbard P.L. & Lewin J. (2016) - Filling the North Sea Basin: Cenozoic sediment sources and river styles (André Dumont medallist lecture 2014). *Geologica Belgica*, 19: 201-217.

Godfrey S.J. & Lambert O. (2023) - Miocene Toothed Whales (Odontoceti) from Calvert Cliffs, Atlantic Coastal Plain, USA. In: Godfrey S.J. (Eds) - The Geology and Vertebrate Paleontology of Calvert Cliffs, Maryland, USA - Volume 2 Turtles and Toothed Whales: 49-186. Smithsonian Institution Scholarly Press, Washington D.C.

Guo Z. & Kohno N. (2023) - An Early Miocene kentriodontoid (Cetacea: Odontoceti) from the western North Pacific, and its implications for their phylogeny and paleobiogeography. *PLoS ONE*, 18: e0280218.

Hartman K.L., Fernandez M. & Azevedo J.M. (2014) - Spatial segregation of calving and nursing Risso's dolphins (*Grampus griseus*) in the Azores, and its conservation implications. *Marine Biology*, 161: 1419-1428.

Ichishima H., Barnes L.G., Fordyce R.E., Kimura M. & Bohaska D.J. (1994) - A review of kentriodontine dolphins (Cetacea; Delphinoidea; Kentriodontidae): Systematics and biogeography. *The Island Arc*, 3: 486-492.

Kazár E. & Hampe O. (2014) - A new species of *Kentriodon* (Mammalia, Odontoceti, Delphinoidea) from the middle/late Miocene of Groß Pampau (Schleswig-Holstein, North Germany). *Journal of Vertebrate Paleontology*, 34: 1216-1230.

Kellogg R. (1927) - *Kentriodon pernix*, a Miocene porpoise from Maryland. *Proceedings of the United States National Museum*, 69: 1-55.

Kidwell S.M., Powars D.S, Edwards L.E. & Vogt P.R. (2015) - Miocene stratigraphy and paleoenvironments of the Calvert Cliffs, Maryland. *The Geological Society of America Field Guide*, 40: 231-279.

Kimura T. & Hasegawa Y. (2019) - A new species of *Kentriodon* (Cetacea, Odontoceti, Kentriodontidae) from the Miocene of Japan. *Journal of Vertebrate Paleontology*, 39: e1566739.

Knox R.W.O.B., Bosch J.H.A., Rasmussen E.S., Heilmann-Clausen C., Hiss M., De Lugt I.R., Kasiński J., King C., Köthe A., Słodkowska B., Standke G. & Vandenberghe N. (2010) - Cenozoic. In: Doornenbal J.C. & Stevenson A.G. (Eds) - Petroleum Geological Atlas of the Southern Permian Basin Area: 211-223. EAGE Publications b.v., Houten.

Laga P. & Louwye S. (coll. Mostaert F.) (2006) - Disused Neogene and Quaternary regional stages from Belgium: Bolderian, Houthalenian, Antwerpian, Diestian, Deurnian, Kasterlian, Kattendijkian, Scladisian, Poederlian, Merksemian and Flandrian. *Geologica Belgica*, 9: 215-224.

Lambert O. (2005) - Review of the Miocene long-snouted dolphin *Priscodelphinus cristatus* du Bus, 1872 (Cetacea, Odontoceti) and phylogeny among eurhinodelphinids. *Bulletin de l'Institut royal des Sciences naturelles de Belgique, Sciences de la Terre*, 75: 211-235.

Lambert O., Bianucci G., Urbina M. & Geisler J.H. (2017) - A new inioid (Cetacea, Odontoceti, Delphinida) from the Miocene of Peru and the origin of modern dolphin and porpoise families. *Zoological Journal of the Linnean Society*, 179: 919-946.

Lambert O., Collareta A., Benites-Palomino A., Di Celma C., Muizon, C. de., Urbina M. & Bianucci G. (2021) - A new small, mesorostrine inioid (Cetacea, Odontoceti, Delphinida) from four upper Miocene localities in the Pisco Basin, Peru. *Papers in Palaeontology*, 7: 1043-1064.

Lambert O., Van Boeckel J., Bosselaers M., Gijsen B., Van Rompaey P. & Everaert S. (2025) - A tiny dolphin (Cetacea, Odontoceti, Kentriodontidae) cranium from the Middle Miocene of the southern North Sea with a rare osteological malformation. *Geologica Belgica*, 28: 79-91.

Louwye S., De Coninck J. & Verniers J. (2000) - Shallow marine Lower and Middle Miocene deposits at the southern margin of the North Sea Basin (northern Belgium): dinoflagellate cyst biostratigraphy and depositional history. *Geological Magazine*, 137: 381-394.

Louwye S., Marquet R., Bosselaers M. & Lambert O. (2010) - Stratigraphy of an Early-Middle Miocene Sequence near Antwerp in northern Belgium (Southern North Sea Basin). *Geologica Belgica*, 13: 269-284.

Louwye S., Deckers J., Verhaegen J., Adriaens J. & Vandenberghe N. (2020) - A review of the lower and middle Miocene of northern Belgium. *Geologica Belgica*, 23: 137-156.

Martin A.R. & da Silva V.M.F. (2004) - River dolphins and flooded forest: seasonal habitat use and sexual segregation of botos (*Inia geoffrensis*) in an extreme cetacean environment. *Journal of zoology*, 263: 295-305.

Marx F.G., Lambert O. & Uhen M.D. (2016) - Cetacean Paleobiology. John Wiley & Sons, Chichester, 319 pp.

Mead J.G. & Fordyce R.E. (2009) - The Therian Skull: a Lexicon with Emphasis on the Odontocetes. *Smithsonian Contributions to Zoology*, 627: 1-248.

Mead J.G. & Potter C.W. (1990) - Natural History of Bottle Nose Dolphins along the Central Atlantic Coast of the United States. In: Leatherwood S. & Reeves R.R. (Eds) - The Bottlenose Dolphin: 165-195. Academic Press, San Diego, CA.

Misonne X. (1958) - Faune du Tertiaire et du Pléistocène inférieur de Belgique: (Oiseaux et Mammifères). *Bulletin de l'Institut royal des Sciences naturelles de Belgique*, 34: 1-36.

Muizon C. de (1988a) - Les relations phylogénétiques des Delphinida (Cetacea, Mammalia). *Annales de Paléontologie*, 74: 159-22.

Muizon C. de (1988b) - Les Vertébrés fossiles de la Formation Pisco (Pérou). Troisième partie: Les Odontocètes (Cetacea, Mammalia) du Miocène. *Travaux de l'Institut français d'Etudes Andines*, 42: 1-244.

Muizon C. de (1993) - Walrus-like feeding adaptation in a new cetacean from the Pliocene of Peru. *Nature*, 365: 745-748.

Muizon C. de, Domning D.P. & Ketten D.R. (2002) - *Odobenocetops peruvianus*, the Walrus-Convergent Delphinoid (Mammalia: Cetacea) from the Early Pliocene of Peru. *Smithsonian Contributions to Paleobiology*, 93: 223-261.

Nobile F., Collareta A., Perenzin V., Fornaciari E., Giusberti L. & Bianucci G. (2024) - Dawn of the Delphinidans: New Remains of *Kentriodon* from the Lower Miocene of Italy Shed Light on the Early Radiation of the Most Diverse Extant Cetacean Clade. *Biology*, 13: 114.

Peredo C.M., Uhen M.D. & Nelson M.D. (2018) - A new kentriodontid (Cetacea: Odontoceti) from the early Miocene Astoria Formation and a revision of the stem delphinidan family Kentriodontidae. *Journal of Vertebrate Paleontology*, 38: e1411357.

Perrin W.F. (1975) - Variation of spotted and spinner porpoise (genus *Stenella*) in the eastern Pacific and Hawaii. *Bulletin of the Scripps Institution of Oceanography*, 21: 1-206.

Pyenson N.D. & Sponberg S.N. (2011) - Reconstructing Body Size in Extinct Crown Cetacea (Neoceti) Using Allometry, Phylogenetic Methods and Tests from the Fossil Record. *Journal of Mammalian Evolution*, 18: 269-288.

Roston R.A. & Roth V.L. (2019) - Cetacean Skull Telescoping Brings Evolution of Cranial Sutures into Focus. *The Anatomical Record*, 302: 1055-1073.

True F.W. (1912) - Description of a new fossil porpoise of the genus *Delphinodon* from the Miocene formation of Maryland. *Journal of the Academy of Natural Sciences of Philadelphia*, 15: 165-194.

Turvey S.T., Pitman R.L., Taylor B.L., Barlow J., Akamatsu T., Barrett L.A., Zhao X., Reeves R.R., Stewart B.S., Wang K., Wei Z., Zhang X., Pusser L.T., Richlen M., Brandon J.R. & Wang D. (2007) - First human-caused extinction of a cetacean species? *Biology letters*, 3: 537-540.

Vanden Broeck E. (1878) - Esquisse géologique et paléontologique des dépôts pliocènes des environs d'Anvers, 2ème partie, Les Sables Moyens et les Sables Supérieurs d'Anvers. G. Mayolez, Bruxelles.

Van Waerebeek K. & Würsig B. (2017) - Dusky Dolphin. In: Würsig B., Thewissen J.G.M. & Kovacs K.M. (Eds) - Encyclopedia of marine mammals: 277-280. Academic Press, London, UK.

Ward L.W. (2008) - Synthesis of paleontological and stratigraphic investigations at the Lee Creek Mine, Aurora, N.C. (1958-2007). In: Ray C.E., Bohaska D.J., Koretsky I.A., Ward L.W. & Barnes L.G. (Eds) - Geology and paleontology of the Lee Creek Mine, North Carolina, IV: 325-436. Virginia Museum of Natural History Special Publication 14, Washington D.C.

Whitmore F.C. Jr. & Kaltenbach J.A. (2008) - Neogene Cetacea of the Lee Creek Phosphate Mine, North Carolina. In: Ray C.E., Bohaska D.J., Koretsky I.A., Ward L.W. & Barnes L.G. (Eds) - Geology and paleontology of the Lee Creek Mine, North Carolina, IV: 181-269. Virginia Museum of Natural History Special Publication 14, Washington D.C.